AWARD NUMBER: W81XWH-19-1-0684

TITLE: Targeted Gold Nanoparticles (AuNPs) for Potent Alpha-Particle Radiotherapy of Brain Cancer

PRINCIPAL INVESTIGATOR: Yang Liu

CONTRACTING ORGANIZATION: Duke University

REPORT DATE: June 2022

TYPE OF REPORT: Final Technical Report

PREPARED FOR: U.S. Army Medical Research and Development Command
Fort Detrick, Maryland 21702-5012

DISTRIBUTION STATEMENT: Approved for public release; distribution is unlimited.

The views, opinions and/or findings contained in this report are those of the author(s) and should not be construed as an official Department of the Army position, policy or decision unless so designated by other documentation.

REPORT DOCUMENTATION PAGE

Form Approved OMB No. 0704-0188

Public reporting burden for this collection of information is estimated to average 1 hour per response, including the time for reviewing instructions, searching existing data sources, gathering and maintaining the data needed, and completing and reviewing this collection of information. Send comments regarding this burden estimate or any other aspect of this collection of information, including suggestions for reducing this burden to Department of Defense, Washington Headquarters Services, Directorate for Information Operations and Reports (0704-0188), 1215 Jefferson Davis Highway, Suite 1204, Arlington, VA 22202-4302. Respondents should be aware that notwithstanding any other provision of law, no person shall be subject to any penalty for failing to comply with a collection of information if it does not display a currently valid OMB control number.
PLEASE DO NOT RETURN YOUR FORM TO THE ABOVE ADDRESS.

1. REPORT DATE	**2. REPORT TYPE**	**3. DATES COVERED**
June 2022	Final Report	15 Aug 2019 – 14 Feb 2022

4. TITLE AND SUBTITLE

Targeted Gold Nanoparticles (AuNPs) for Potent Alpha-Particle Radiotherapy of Brain Cancer

5a. CONTRACT NUMBER

5b. GRANT NUMBER
W81XWH-19-1-0684

5c. PROGRAM ELEMENT NUMBER

5d. PROJECT NUMBER

5e. TASK NUMBER

5f. WORK UNIT NUMBER

6. AUTHOR(S)

Yang Liu

E-Mail: yang.liu3@duke.edu

7. PERFORMING ORGANIZATION NAME(S) AND ADDRESS(ES)

Duke University
2200 W Main St STE 710
Durham, NC 27708-4677

8. PERFORMING ORGANIZATION REPORT

9. SPONSORING / MONITORING AGENCY NAME(S) AND ADDRESS(ES)

U.S. Army Medical Research and Development Command

Fort Detrick, Maryland 21702-5012

10. SPONSOR/MONITOR'S ACRONYM(S)

11. SPONSOR/MONITOR'S REPORT NUMBER(S)

12. DISTRIBUTION / AVAILABILITY STATEMENT

Approved for Public Release; Distribution Unlimited

13. SUPPLEMENTARY NOTES

14. ABSTRACT

Glioblastoma (GBM) is the most common and aggressive brain cancer. Even with the highest first-year cost (> $120,000), the prognosis for GBM patients is dismal. Therefore, it is of great clinical significance to develop novel therapeutic approaches to improve GBM treatment efficacy. Alpha particle radiation therapy with high linear energy transfer (80 keV/μm) has a potent therapeutic effect independent of dose rate, cell cycle, and oxygen concentration. A single alpha-particle track can result in lethal DNA double-strand breaks. Astatine-211 (^{211}At) is an attractive alpha emitter for alpha particle radiation therapy because it has the advantages of an optimal half-life (7.2 h) and no long-lived decay "daughter" radionuclides thus avoiding toxicity from daughter radionuclide redistribution. However, traditional ^{211}At radiolabeling methods have the challenges of a complicated radiolabeling process and low conjugation efficiency. In this study, we develop targeted gold nanoparticles as a novel ^{211}At delivery nanoplatform for alpha particle radiation therapy. We have demonstrated that the developed gold nanoparticles can selectively accumulate in the brain tumor. We also performed preliminary in vivo toxicity study and therapeutic efficacy test. Experiment results demonstrated that ^{211}At-loaded gold nanoparticles can substantially reduce tumor growth after intratumoral administration using a murine animal model.

15. SUBJECT TERMS

Brain Cancer, Nanoparticles, At-211 alpha particle radiation therapy.

16. SECURITY CLASSIFICATION OF:			**17. LIMITATION OF ABSTRACT**	**18. NUMBER OF PAGES**	**19a. NAME OF RESPONSIBLE PERSON** USAMRDC
a. REPORT	**b. ABSTRACT**	**c. THIS PAGE**	UU	**34**	**19b. TELEPHONE NUMBER** *(include area code)*
U	U	U			

TABLE OF CONTENTS

1. **INTRODUCTION:** *Narrative that briefly (one paragraph) describes the subject, purpose and scope of the research.*

Glioblastoma (GBM) is one of the most common and aggressive brain cancer with more than 10,000 newly diagnosed patients in the United States each year. The median survival is only 15 months even after aggressive treatments including surgery, chemotherapy, and radiation therapy. There is a clear and urgent need to develop novel therapeutic approaches for effective GBM treatment. Alpha particle radiation therapy has the promise to improve brain cancer treatment with its potent cytotoxicity from high linear energy transfer. Among different available alpha-particle emitters, astatine-211 (^{211}At) has the advantage of optimal half-life (7.2 h) and no confounding radioactive daughters. This project is aimed to develop targeted gold nanoparticles as a novel ^{211}At delivery platform to treat brain cancer using murine animal models.

2. **KEYWORDS:** *Provide a brief list of keywords (limit to 20 words).*

Brain Cancer, Glioblastoma (GBM), Alpha particle radiation therapy, Astatine-211 (^{211}At), Gold nanoparticles (AuNPs).

3. **ACCOMPLISHMENTS:** *The PI is reminded that the recipient organization is required to obtain prior written approval from the awarding agency grants official whenever there are significant changes in the project or its direction.*

What were the major goals of the project?

List the major goals of the project as stated in the approved SOW. If the application listed milestones/target dates for important activities or phases of the project, identify these dates and show actual completion dates or the percentage of completion.

Major goal 1: Develop AuNPs for At-211 alpha particle radiation therapy.

Milestone 1.1: Obtain AuNPs with different sizes for radiolabeling. (Target date: Dec 14th, 2019; 100% completed).

Milestone 1.2: Get optimized AuNPs with high radiolabeling efficiency. (Target date: May 14th, 2020; 100% completed).

Major goal 2: Functionalize AuNPs for brain cancer targeting and treatment.

Milestone 2.1: Functionalize AuNPs with both c(RGDfK) and angiopep-2 ligands. (Target date: May 14th, 2020; 100% completed)

Milestone 2.2: Characterize AuNP's properties (Target date: May 14th, 2020; 80% completed).

Milestone 2.3: Demonstrate developed AuNPs can target and treat brain cancer cells with in vitro test (Target date: August 14th, 2020; 70% completed).

Major goal 3: Evaluate brain cancer targeting, pharmacokinetics, and therapeutic effect of developed AuNPs using murine animal models.

Milestone 3.0: Get animal protocol approved by Duke IACUC and DOD ACURO. (Target date: November 14th, 2019; 100% completed)

Milestone 3.1: Get in vivo biodistribution and pharmacokinetic properties of AuNPs. (Target date: Nov 14th, 2020; 100% completed)

Major goal 3.2: Obtain MTD of ^{211}At-AuNPs. (Targeted date: November 14th, 2020; 100% completed)

Major goal 3.3: Determine the therapeutic effect of the developed ^{211}At alpha-particle radiotherapy with AuNPs and prepare a manuscript for publication. (Targeted date: February 14th, 2021; 100% completed)

What was accomplished under these goals?

For this reporting period describe: 1) major activities; 2) specific objectives; 3) significant results or key outcomes, including major findings, developments, or conclusions (both positive and negative); and/or 4) other achievements. Include a discussion of stated goals not met. Description shall include pertinent data and graphs in sufficient detail to explain any significant results achieved. A succinct description of the methodology used shall be provided. As the project progresses to completion, the emphasis in reporting in this section should shift from reporting activities to reporting accomplishments.

Aim 1. Synthesize, optimize and evaluate AuNPs (< 5 nm) for ^{211}At and ^{124}I labeling

Major task 1: Synthesize AuNPs with size between 1 and 5 nm

We synthesized different gold nanoparticles for ^{211}At and ^{124}I labeling. Transmission electron microscopy and dynamic light scattering were used to characterize the synthesized 3 nm AuNPs (**Figure 1A**) and 12 nm AuNPs (**Figure 1B**). 3 nm AuNPs were synthesized by reducing $HAuCl_4$ with $NaBH_4$ in the presence of SH-PEG_6 and SH-PEG_8-COOH in the ice-cooled water solution. The synthesized AuNPs were measured to have similar hydrodynamic size as that of 13 KDa protein (**Figure 1C**) using size exclusion chromatography. The 12 nm AuNPs were synthesized by reducing $HAuCl_4$ with sodium citrate in the boiling water. The obtained AuNPs in different sizes were used for the following radiolabeling studies.

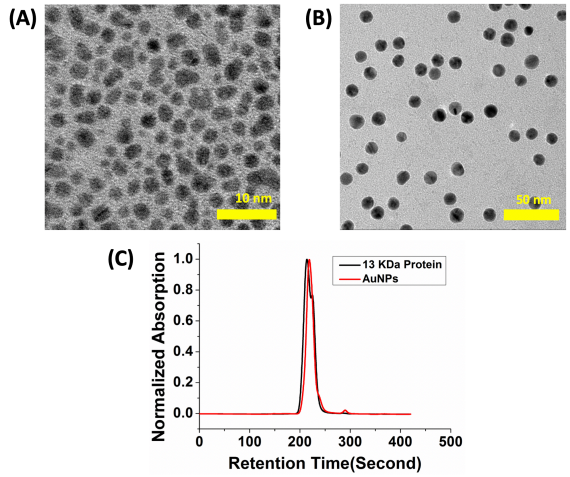

Figure 1. TEM image for the synthesized 3 nm AuNPs (A) and 12 nm AuNPs (B). Size exclusion chromatography for the synthesized 3 nm AuNPs (C). 13 KDa protein was used as a standard.

Major task 2: Evaluate ^{211}At and ^{124}I labeling on AuNPs with different size

^{211}At radioisotopes were produced using CS-30 cyclotron at Duke University. The ^{211}At radioisotopes generated on the bismuth target were collected by using dry distillation method. The obtained ^{211}At radioisotopes in methanol were used for the following studies.

First, we used 3 nm AuNPs to test radiolabeling efficiency with ^{211}At in different oxidation state (-1, 0 and +1). After half-hour incubation, the radiolabeling efficiency was determined to be 97.6%, 96.4% and 89.2% for ^{211}At at -1, 0, and +1 oxidation state, respectively. We performed quantum chemistry calculation to investigate bonding mechanism and found the At-Au bond contained 19% 5P:z atomic orbital, 36% 6S atomic orbital of At and 44% 3D:z^2 atomic orbital of Au (**Figure 2**). The valence state for At and Au was determined to be -1 and +1 respectively.

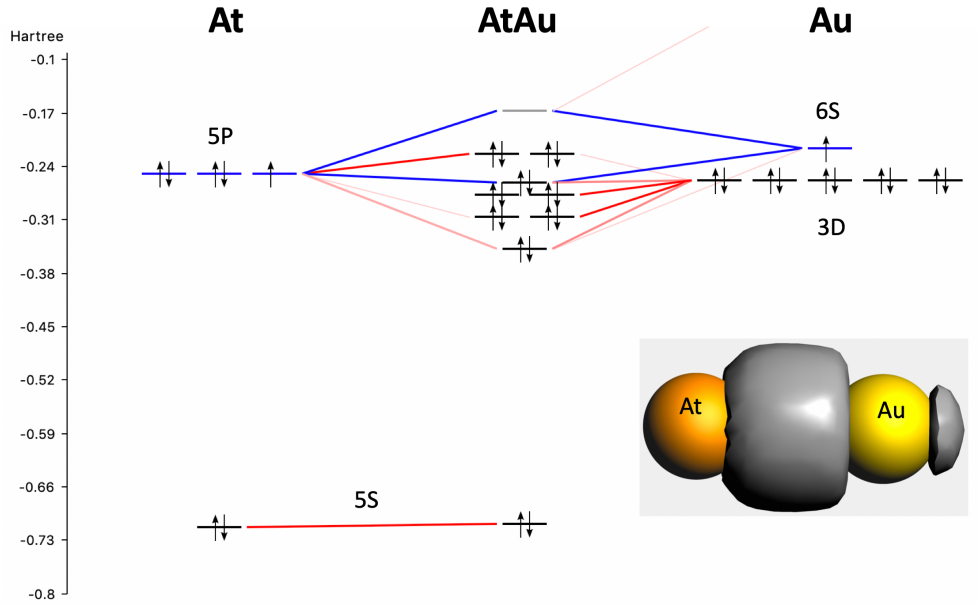

Figure. 2. Bonding mechanism analysis for At-Au chemical bond. Amsterdam Density Functional (ADF) software was used to perform quantum chemistry calculation.

Second, we used 3 nm AuNPs to test how incubation time and Au mass affect ^{211}At (-1 state) radiolabeling efficiency. The Au mass for test was 200 µg in 200 µl solution. The radiolabeling efficiency at room temperature was measured to be 94%, 97%, and 98% for 1 min, 5 min, and 30 min incubation time, respectively. After that, we tested how Au mass affects ^{211}At radiolabeling efficiency with 5 min incubation at room temperature. The measured efficiency is 97% (200 µg), 90% (20 µg), 85% (2 µg), 76% (200 ng), 58% (20 ng), 10% (2 ng), respectively. Experiment results demonstrated that the synthesized 3 nm AuNPs could reach high radiolabeling efficiency by simply incubating AuNPs with At-211 for 5 minutes at room temperature.

Third, we performed ^{211}At stability test in different challenge conditions. The ^{211}At radioactivity remaining on AuNPs was measured to be 96% (smashed liver suspension water solution), 98% (murine serum), and 99% (phosphate buffered saline) after 3 hours incubation at 37 °C. Phantom studies demonstrated that the synthesized 3 nm AuNPs could load ^{211}At with high stability. 12 nm AuNPs had similar performance for ^{211}At radiolabeling and stability tests.

We also tested 3 nm AuNP's radiolabeling performance for iodine radioisotopes (^{131}I). The radiolabeling efficiency was measured to be 99% (200 µg Au, 5 min incubation at room temperature) and 71% (2 µg Au, 5 min incubation at room temperature). Density functional theory calculation was performed to investigate the bonding mechanism of Au-I chemical bond. We found the Au-I bond contained 19% 4P:z atomic orbital of I and 36% 6S atomic orbital and 44% 3D:z^2 atomic orbital of Au (**Figure 3**). The oxidation state for I and Au was determined to be -1 and +1 respectively. The bonding mechanism of Au-I is similar as that of Au-At.

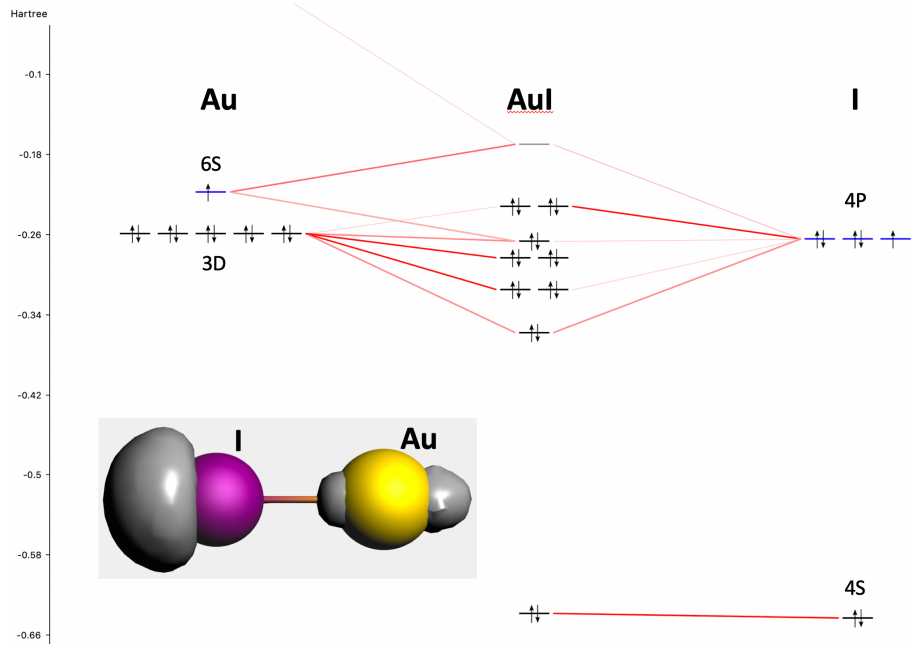

Figure. 3. Bonding mechanism analysis for At-I chemical bond. Amsterdam Density Functional (ADF) software was used to perform quantum chemistry calculation.

Aim 2. Conjugate AuNPs with tumor-homing peptides for brain cancer-targeting and perform *in vitro* tests to demonstrate the developed nanoagent can target and treat brain cancer.

Major task 1: Functionalize AuNPs with brain cancer targeting ligands and peptides for blood-brain-barrier penetration.

We conjugated c(RGDfK) peptide to 3 nm AuNPs by using Amine-NHS chemistry method. The 3 nm AuNPs had carboxylic acid functional group at the end of SH-PEG_8 chain. The carboxylic acid group was converted to N-hydroxysuccinimide (NHS) ester by using 1-ethyl-3-(3-dimethylaminopropyl)carbodiimide (EDC) and Sulfo-NHS. After that, the free amine group in the c(RGDfK) side chain was used to react with NHS ester for conjugation. In addition, we also functionalized 3 nm AuNPs with angiopep-2. The custom-synthesized peptide had a cystine on the end, which was used to bind to AuNPs. Angiopep-2 peptide could help AuNPs penetrate blood-brain-barrier by low-density lipoprotein receptor-mediated transcytosis. We have developed AuNPs functionalized with both c(RGDfK) and angiopep-2 peptides.

Major task 2: Characterize synthesized AuNPs and quantify ligands number per AuNP nanoparticle.

We characterized AuNPs with transmission electron tomography, dynamic light scattering, and size exclusion chromatography (Figure. 1.). We also used inductively coupled plasma mass spectrometry (ICP-MS) to measure gold mass of synthesized AuNPs. And we tried to use liquid chromatography-mass spectrometry (LC-MS) to quantify the targeting ligand number per AuNPs. However, the AuNPs functionalized with c(RGDfK) peptide were not stable in the phosphate buffered saline solution and got aggregated quickly. A possible reason is that functionalized c(RGDfK) peptide is hydrophobic, making AuNPs unstable in the aqueous solution. As a result, we will use PEG functionalized AuNPs for following in vivo studies.

Major task 3: Perform *in vitro* evaluation of the binding behavior and cytotoxicity of targeted ^{211}At-AuNPs using U87MG brain cancer cell line from ATCC.

We tried to use U87MG brain cancer cells to perform in vitro cell binding studies for c(RGDfK)-functionalized AuNPs. c(RGDfK) peptide has a high binding affinity of 2 nM to αVβ3 receptors overexpressed on brain cancer and its neovasculature cells. However, the AuNPs functionalized with c(RGDfK) peptide were not stable in the 1X phosphate buffered saline solution and got aggregated quickly. A possible reason is that functionalized c(RGDfK) peptide is hydrophobic, making AuNPs unstable in aqueous solution. As a result, we will use PEG functionalized AuNPs for following in vivo studies.

Aim 3: Evaluate *in vivo* brain cancer targeting, pharmacokinetics, and therapeutic effect of targeted AuNPs labeled with both ^{211}At and ^{124}I.

Major task 1: Investigate brain cancer uptake, biodistribution and pharmacokinetics of targeted AuNPs by microPET/CT imaging and using GBM brain tumor model with U87MG brain cancer cells from ATCC.

We performed in vivo biodistribution studies for the synthesized AuNPs. For 3 nm AuNPs, we did in vivo biodistribution study for both ^{211}At and ^{131}I radiolabeling 1h, 4h, and 24h after intravenous (IV) injection through tail vein. For ^{211}At radiolabeled 3 nm AuNPs (**Table 1**), high radioactivity was found in the urine 1 h after IV injection. Bladder and stomach were organs with high uptake. Thyroid had moderate uptake which changed from 5.32 %ID/g at 1h to 9.44 %ID/g at 24h. The biodistribution results might indicate ^{211}At radioisotopes leached out of 3 nm AuNPs and got cleared quickly by urine.

Table 1. In vivo biodistribution of ^{211}At-loaded 3 nm AuNPs 1h, 4h and 24h after intravenous injection. Sm. Int. is short for small intestine and Lg. Int. is short for large intestine. %ID/g is defined as the percent injection dose per gram tissue. SD, standard deviation (n=4).

^{211}At-3nm AuNPs	1h		4h		24h	
%ID/g	Mean	SD	Mean	SD	Mean	SD
Liver	1.39	0.05	1.56	0.22	0.51	0.15
Spleen	2.91	0.63	3.96	1.59	0.44	0.42
Lung	9.41	3.70	7.06	1.33	0.67	0.33
Heart	1.61	0.48	1.82	0.20	0.15	0.15
Kidney	1.99	0.25	1.76	0.30	0.22	0.08
Bladder	29.02	15.52	4.33	2.24	0.15	0.47
Stomach	21.46	9.68	27.95	14.00	2.72	1.59
Sm. Int.	2.17	0.24	1.58	0.32	0.18	0.03
Lg. Int.	1.09	0.14	0.95	0.23	0.15	0.09
Thyroid	5.32	2.11	5.73	1.13	9.44	4.03
Blood	1.23	0.06	0.98	0.22	0.08	0.02
Urine	262.27	195.02	73.23	69.55	3.29	2.11
Skin	2.15	1.23	1.87	0.56	0.32	0.04
Brain	0.19	0.05	0.17	0.06	0.02	0.08

For ^{131}I-loaded 3 nm AuNPs (**Table 2**), high radioactivity was also found in the urine 1h after IV injection. Stomach, bladder, and thyroid were organs with high radioactivity. The biodistribution study results could indicate that ^{131}I radioisotopes leached out of 3 nm AuNPs after IV injection.

Table 2. In vivo biodistribution of ^{131}I-loaded 3 nm AuNPs 1h, 4h and 24h after intravenous injection. Sm. Int. is short for small intestine and Lg. Int. is short for large intestine. %ID/g is defined as the percent injection dose per gram tissue. SD, standard deviation (n=4).

^{131}I-3nm AuNPs	1h		4h		24h	
%ID/g	Mean	SD	Mean	SD	Mean	SD
Liver	1.55	0.14	0.94	0.41	0.03	0.01
Spleen	1.35	0.27	0.62	0.28	0.00	0.01
Lung	2.77	0.74	1.41	0.47	0.01	0.01
Heart	1.36	0.41	0.83	0.37	0.00	0.01
Kidney	1.97	0.57	1.22	0.57	0.02	0.01
Bladder	12.01	7.78	2.13	1.34	0.00	0.04
Stomach	48.03	26.32	30.54	20.94	0.30	0.14
Sm. Int.	4.50	1.46	1.56	0.73	0.02	0.01
Lg. Int.	1.57	0.20	2.33	1.20	0.02	0.01
Thyroid	27.78	14.89	16.88	6.85	5.57	3.81
Blood	3.76	1.20	2.08	0.77	0.02	0.01
Urine	104.54	64.11	48.77	35.42	1.29	1.25
Skin	2.59	1.11	1.43	0.47	0.10	0.03
Brain	0.16	0.05	0.08	0.04	0.00	0.00

We also performed in vivo biodistribution study for ^{211}At-labeled 12 nm spherical AuNPs. As shown in the **Table 3**, high radioactivity was found in blood but not urine 1h after IV injection. The radioactivity in blood decreased from 44.22 %ID/g at 1h to 16.33 %ID/g at 24h. Both thyroid and stomach had low radioactivity. The biodistribution results showed that ^{211}At was stable on 12 nm spherical AuNPs after IV injection. In addition, ^{211}At-labeled 12 nm spherical AuNPs were found not to be cleared out of the body by kidney and had a long blood circulation time.

In addition, we radiolabeled 50 nm star-shaped AuNPs with ^{124}I and performed microPET/CT scan to investigate brain cancer uptake, biodistribution, and pharmacokinetics with the developed murine intracranial brain tumor model using U87MG brain cancer cells. The radiolabeling process was performed by mixing ^{124}I with star-shaped AuNPs. The radiolabeled AuNPs were purified by centrifugation wash and radiolabeling efficiency are more than 95% by simply incubating in water solution for 5 mins. For PET/CT scan, radiolabeled star-shaped AuNPs were injected through tail vein and mice with brain tumor were imaged 10 min, 4 h, 24 h, 48 h, and 120 h after injection. Gold nanoparticles were found in brain tumor part but not surrounding healthy brain tissue (**Figure 4**).

Table 3. In vivo biodistribution of ^{211}At-loaded 12 nm spherical AuNPs 1h, 4h and 24 h after intravenous injection. Sm. Int. is short for small intestine and Lg. Int. is short for large intestine. %ID/g is defined as the percent injection dose per gram tissue. SD, standard deviation (n=3).

^{211}At-12 nm AuNPs	1 h		4 h		24 h	
%ID/g	mean	SD	mean	SD	mean	SD
Liver	9.79	1.43	10.86	2.09	12.27	1.08
Spleen	4.83	1.70	7.44	0.47	16.92	3.45
Lung	17.54	3.24	15.18	2.23	6.23	2.91
Heart	9.82	1.87	9.44	2.13	5.50	0.94
Kidney	9.45	1.07	9.13	1.13	5.84	0.32
Bladder	2.21	0.39	2.54	0.96	2.90	0.66
Stomach	4.96	1.03	4.83	0.86	2.53	0.38
Sm. Int.	2.23	0.40	2.37	0.56	1.51	0.18
Lg. Int.	0.73	0.19	0.94	0.19	0.72	0.20
Thyroid	5.14	1.09	5.41	0.74	2.84	0.82
Blood	44.22	6.22	41.21	4.89	16.33	0.80
Urine	1.53	0.65	2.52	2.18	2.79	0.72
Tumor	0.00	0.00	0.00	0.00	0.00	0.00
Skin	2.15	0.50	2.86	0.74	3.81	0.79
Brain	1.51	0.21	1.25	0.26	0.64	0.03

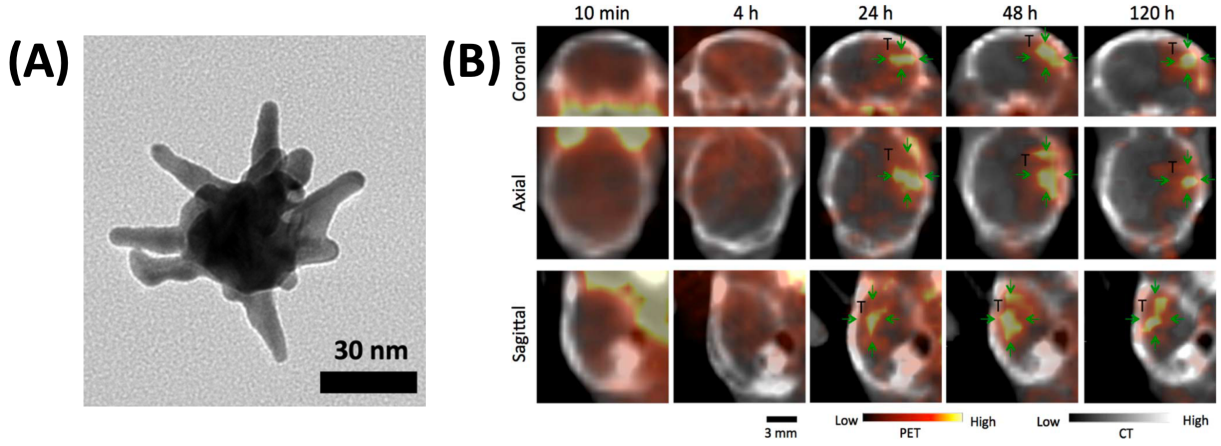

Figure 4. (A) TEM imaging of developed 50-nm star-shaped AuNPs. (B) PET/CT imaging of I-124 labeled star-shape AuNPs in the intracranial brain tumor 10 min, 4 h, 24 h, 48 h, and 120 h after intravenous injection. Top, middle and bottom rows show coronal, axial and sagittal image, respectively. Significantly higher ^{124}I-AuNPs uptake in tumor (T; green arrows) compared with contralateral normal brain was observed at 24 h.

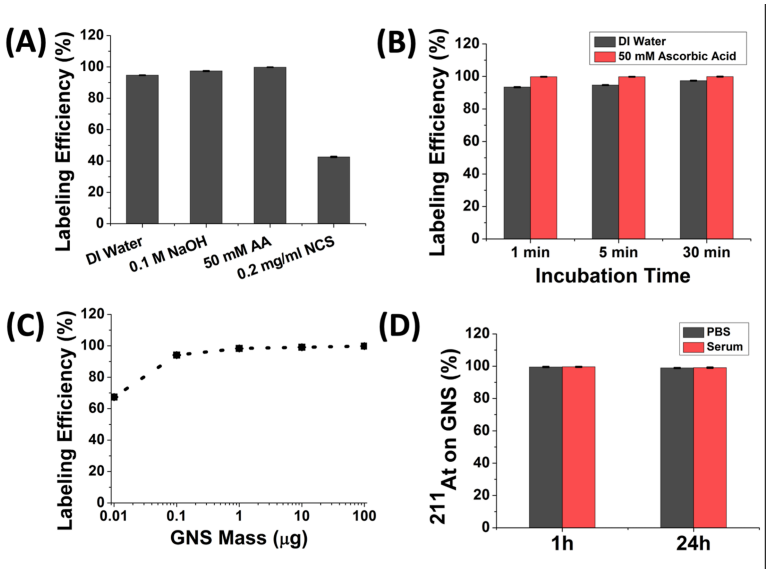

Figure 5. Evaluation of radiolabeling star-shaped AuNPs with ^{211}At. (A). Radiolabeling efficiency evaluation in different reaction solutions: Deionised (DI) water, DI water with 0.1 M NaOH, DI water with 50 mM ascorbic acid, DI water with 0.2 mg/ml N-chlorosuccinimide (NCS) after a 5 min incubation. (B) Radiolabeling efficiency as a function of incubation time when the reaction was performed using DI water or DI water with 50 mM ascorbic acid as the media. (C) Radiolabeling efficiency evaluation for star-shaped AuNPs (GNS) mass ranging from 0.01-100 μg for 5 min incubation in DI water with 50 mM ascorbic acid. (D) Percentage of ^{211}At remaining on star-shaped AuNPs after incubation in PBS and murine serum at 37ºC for 1 h and 24 h. All experiments performed in triplicate and error bar shows standard deviation.

We performed At-211 radiolabeling experiments using PEGylated star-shaped AuNPs and the results are shown in **Figure 5**. First, we compared the radiolabeling efficiency in four different reaction solutions. The calculated At-211 labeling efficiency was 94.7 ± 0.1% in DI water, 97.4 ± 0.2% in DI water with 0.1 M NaOH, 99.8 ± 0.1% in deionized (DI) water with 50 mM ascorbic acid, and 42.6 ± 0.3% in DI water with 0.2 mg/ml N-chlorosuccinimide (NCS). The radiolabeling efficiency for the reaction medium with a reducing agent, ascorbic acid, was the highest (99.8%), and almost all the At-211 could be attached to star-shaped AuNPs after only a 5-min incubation at room temperature. Conversely, the NCS oxidizing agent dramatically decreased the radiolabeling efficiency to 42.6 ± 0.3%. Second, we evaluated the effect of incubation time on radiolabeling efficiency in reaction media consisting of DI water or DI water with 50 mM ascorbic acid. The radiolabeling efficiency in DI water increased from 93.4 ± 0.2% (1 min), to 94.7 ± 0.1% (5 min), and 97.4 ± 0.2% (30 min). The radiolabeling efficiency in DI water with 50 mM ascorbic acid was essentially quantitative by 1 min and remained constant over 30 min. Third, we compared how the nanoparticle-to-^{211}At ratio affected the radiolabeling using DI water with 50 mM ascorbic acid as the reaction medium. The radiolabeling efficiency decreased as the ^{211}At:AuNP ratio increased: from 99.8 ± 0.1 % (540 fmol AuNPs, ^{211}At:AuNP = 0.85), 99.1 ± 0.1% (54 fmol AuNPs, ^{211}At:AuNP = 8.5), 98.3 ± 0.1% (5.4 fmol AuNPs, ^{211}At:AuNP = 85), 94.1 ± 0.2% (540 amol AuNPs, ^{211}At:AuNP = 850), and 67.4 ± 0.2% (54 amol AuNPs, ^{211}At:AuNP = 8,500). The in vitro stability tests at 37°C indicated that 99.5 ± 0.3% and 99.6 ± 0.2% ^{211}At remained on star-shaped AuNP after 1 h incubation in PBS and serum, respectively. After 24 h incubation, the percentage of ^{211}At on star-shaped AuNP was 98.9 ± 0.2% for PBS and 99.1 ± 0.3% for serum at 37°C.

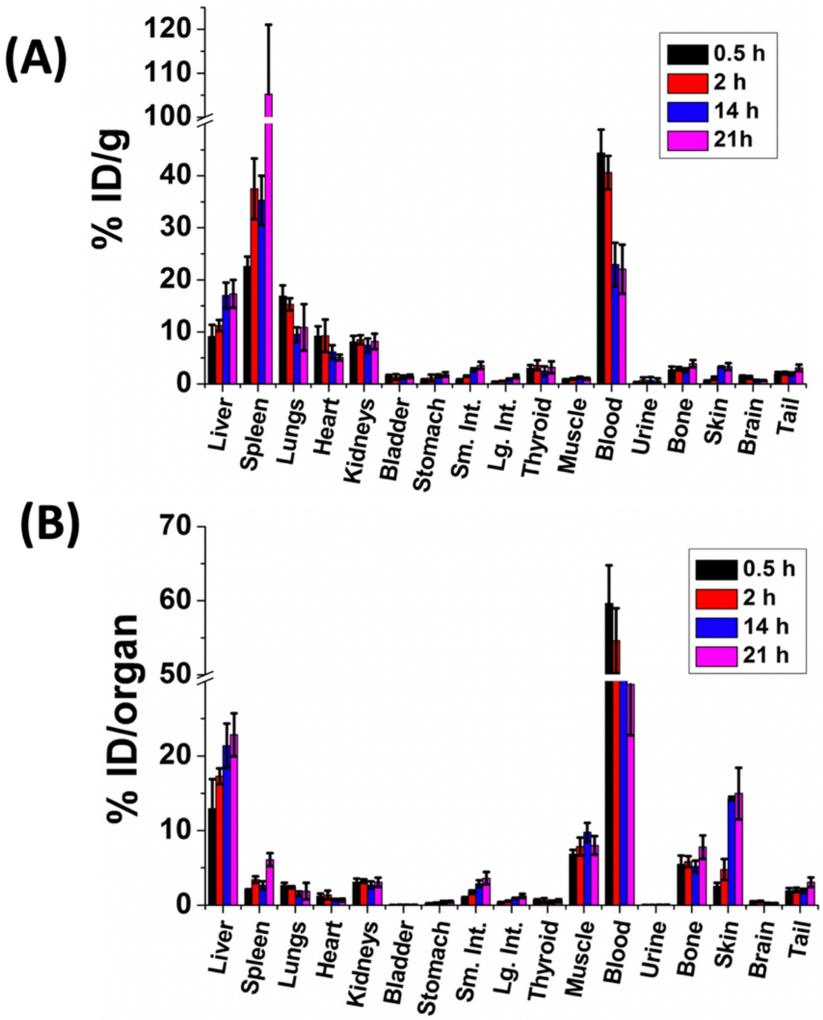

Figure 6. In vivo biodistribution of ^{211}At activity after intravenous injection of ^{211}At-labeled 50-nm star-shaped AuNPs in normal mice. The results are shown as percent injected dose per gram tissue (%ID/g) [Figure (A)], and as percent injected dose per organ (%ID/organ) [Figure (B)]. Error bar shows the standard deviation (n=5).

In addition, we performed in vivo biodistribution study for ^{211}At radiolabeled 50-nm star-shaped AuNPs after intravenous injection. 4 time points were studied (0.5 h, 2 h, 14 h, and 21 h). The radiolabeling efficiency of ^{211}At on star-shaped AuNPs was almost 100% using a simple and rapid synthesis process that was completed in only 1 min. As shown in **Figure 6**, *in vivo* biodistribution results demonstrated low uptake in the thyroid (0.44-0.64 %ID) and stomach (0.21-0.49 %ID) between 0.5 h and 21 h after intravenous injection, thus indicating excellent *in vivo* stability of ^{211}At-labeled gold nanoparticles. Since 50-nm star-shaped AuNPs have the best radiolabeling and in vivo stability performance among 3 tested AuNPs in this study, we will use 50-nm star-shaped AuNPs for the following in vivo toxicity and therapeutic efficacy studies.

Major task 2: Determine the maximum tolerated dose (MTD) of ^{211}At-AuNPs.

We performed preliminary *in vivo* toxicity study to determine the MTD of ^{211}At radiolabeled gold nanoparticles after intravenous injection. 3 doses of ^{211}At (0.3 mCi/kg, 1 mCi/kg, and 4 mCi/kg) were tested. 50-nm star-shaped AuNPs without ^{211}At were used as control. As shown in the **Figure 7**, 3 of 5 mice died within 9 days after IV injection of 4 mCi/kg ^{211}At radiolabeled 50-nm star-shaped AuNPs. For the 1mCi/kg group, 2 of 5 mice died within 9 days after IV injection. For the 0.3 mCi/kg group, none of the mice died and the body weight has no obvious decrease.

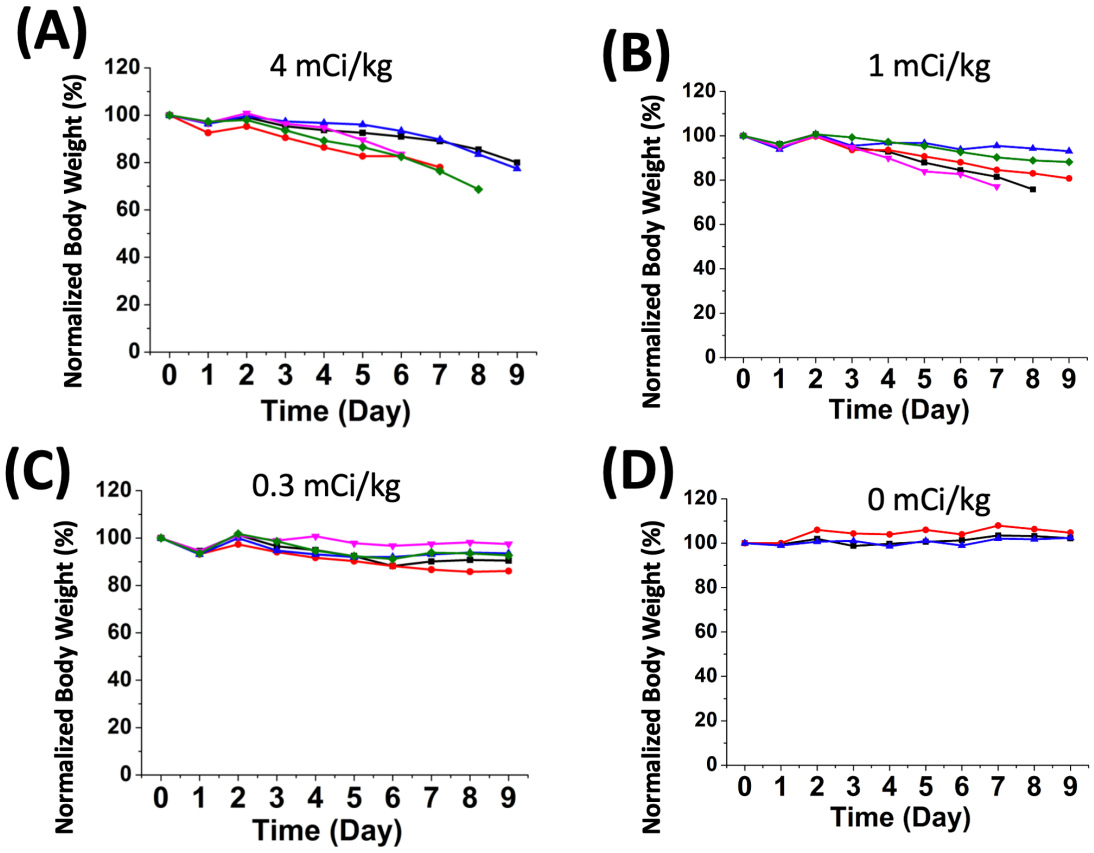

Figure 7. Body weight monitoring for mice with systemic administration of ^{211}At labeled 50-nm star-shaped AuNPs through tail vein. The ^{211}At dose ranging from 0.3 mCi/kg to 4 mCi/kg were tested. The body weight for mice with the 0.3 mCi/kg dose shows minimal body weight decrease.

Major task 3: Determine therapeutic response for targeted ^{211}At-AuNPs using GBM murine animal model with nude mice and U87MG cell line.

We performed a preliminary evaluation on the therapeutic efficacy of ^{211}At-labeled 50-nm star-shaped AuNPs. The experiment was performed in athymic mice with subcutaneous U87MG human glioma xenografts with the labeled drug given by the intratumoral route. As shown in the **Figure 8**, the ^{211}At-labeled 50-nm star-shaped AuNPs substantially inhibited the tumor growth rate. The average tumor volume in the control group increased rapidly from 82 mm^3 on Day 1 to 177 mm^3, 409 mm^3, 798 mm^3, and 1456 mm^3 on Days 4, 7, 10, and 14, respectively. In contrast, the average tumor volume in the treatment group increased slowly, from 78 mm^3 on Day 1 to 95 mm^3, 112 mm^3, 152 mm^3, and 189 mm^3 on Days 4, 7, 10, and 14, respectively. The two-way ANOVA test indicated that the difference in tumor volumes between the ^{211}At-labeled AuNPs treated group and the control group with PBS injection was statistically significant (P<0.001).

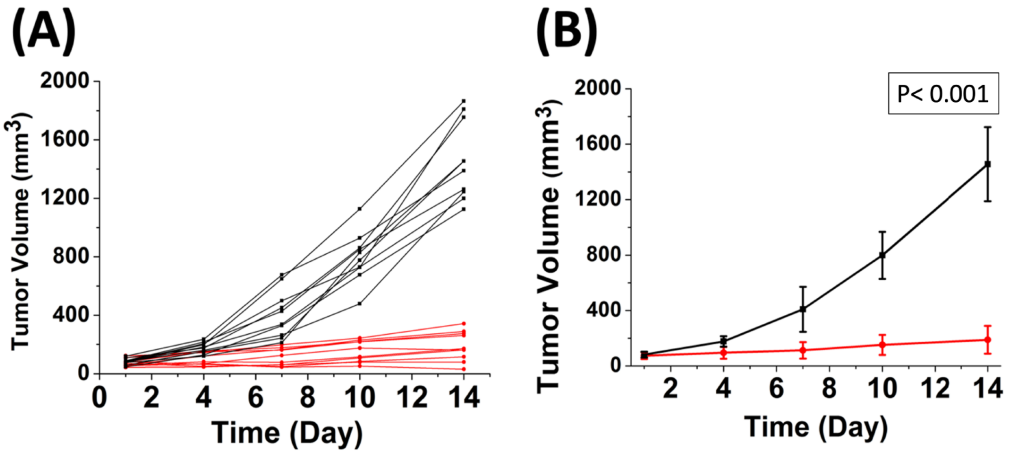

Figure 8. Therapeutic efficacy evaluation of ^{211}At therapy using 50-nm star-shaped AuNPs as a novel delivery platform. (A) tumor size change profile for each mouse in the ^{211}At-AuNPs treatment group (1.11 MBq, red color line) and blank control group with PBS injection (black color line). (B) Average tumor size change profile for mice in the ^{211}At-AuNPs treatment group (1.11 MBq, red color line) and blank control group with PBS injection (Black color line). Error bar shows standard deviation (n = 10). P value was calculated using 2-way ANOVA (P< 0.001).

Summary

In summary, we have developed targeted AuNPs with high ^{211}At loading capability for alpha particle radiation therapy to treat brain cancer. Furthermore, we have performed in vivo studies to investigate the brain cancer uptake, biodistribution, and therapeutic efficacy of AuNPs loaded with ^{211}At. Preliminary results demonstrated that the ^{211}At radiolabeled AuNPs could reduce tumor growth using a brain cancer murine animal model.

What opportunities for training and professional development has the project provided?
If the project was not intended to provide training and professional development opportunities or there is nothing significant to report during this reporting period, state "Nothing to Report."

Describe opportunities for training and professional development provided to anyone who worked on the project or anyone who was involved in the activities supported by the project. "Training" activities are those in which individuals with advanced professional skills and experience assist others in attaining greater proficiency. Training activities may include, for example, courses or one-on-one work with a mentor. "Professional development" activities result in increased knowledge or skill in one's area of expertise and may include workshops, conferences, seminars, study groups, and individual study. Include participation in conferences, workshops, and seminars not listed under major activities.

The Horizon award has provided me precious opportunities to take training as a radiochemist on ^{211}At production, processing, purification and radiolabeling. I have also learned how to perform in vitro cell studies and in vivo animal studies. I have met my research mentors, Professor Tuan Vo-Dinh and Professor Michael Zalutsky, weekly to discuss project progress and received their professional comments and suggestions. Besides, I attended a virtual webinar-style meeting held by the National Isotope Development Center (NIDC) of the U.S. Department of Energy (DOE) focusing on Astatine-211 generation and biomedical applications. I attended the conference Pacifichem 2021 for the symposium entitled "Advancements in the Chemistry of Targeted Alpha Therapy" to learn latest advancements in alpha particle radiation therapy using Astatine-211 and other alpha emitters.

How were the results disseminated to communities of interest?
If there is nothing significant to report during this reporting period, state "Nothing to Report."

Describe how the results were disseminated to communities of interest. Include any outreach activities that were undertaken to reach members of communities who are not usually aware of these project activities, for the purpose of enhancing public understanding and increasing interest in learning and careers in science, technology, and the humanities.

I have published a paper in the International Journal of Nanomedicine with the title of "Gold nanostars: A novel platform for developing ^{211}At-labeled agents for targeted alpha-particle therapy" to disseminate the results to communities of interest. The published paper is shown in the attachment.

In addition, I also submitted an abstract for the conference Pacifichem 2021 with the title of "Gold nanoparticles as a novel delivery strategy for targeted alpha therapy". The abstract has been accepted for an oral presentation to disseminate the results to communities of interest. I attended the conference between December 16, 2021 and December 21, 2021. The abstract is shown in the attachment.

Describe briefly what you plan to do during the next reporting period to accomplish the goals and objectives.

This is not applicable because the report is final.

4. **IMPACT:** D*escribe distinctive contributions, major accomplishments, innovations, successes, or any change in practice or behavior that has come about as a result of the project relative to:*

What was the impact on the development of the principal discipline(s) of the project?
If there is nothing significant to report during this reporting period, state "Nothing to Report."

Describe how findings, results, techniques that were developed or extended, or other products from the project made an impact or are likely to make an impact on the base of knowledge, theory, and research in the principal disciplinary field(s) of the project. Summarize using language that an intelligent lay audience can understand (Scientific American style).

From this project, we demonstrated that AuNPs can be used as a novel delivery platform for ^{211}At alpha particle radiation therapy. The developed strategy has the advantages of the simple radiolabeling process, high conjugation efficiency and in vivo stability, which is attractive for targeted alpha particle therapy to treat cancer.

What was the impact on other disciplines?
If there is nothing significant to report during this reporting period, state "Nothing to Report."

Describe how the findings, results, or techniques that were developed or improved, or other products from the project made an impact or are likely to make an impact on other disciplines.

We are first to explore gold nanoparticles as a novel ^{211}At carrier for in vivo cancer treatment. Preliminary results demonstrated that ^{211}At labeled gold nanoparticles can substantially reduce brain cancer growth. The optimized gold nanoparticles with high ^{211}At binding affinity and in vivo stability may serve as a novel delivery strategy for alpha particle radiation therapy to treat aggressive cancer.

What was the impact on technology transfer?
If there is nothing significant to report during this reporting period, state "Nothing to Report."

Describe ways in which the project made an impact, or is likely to make an impact, on commercial technology or public use, including:

- *transfer of results to entities in government or industry;*
- *instances where the research has led to the initiation of a start-up company; or*
- *adoption of new practices.*

The delivery nanoplatform developed in this project has the promise to make an impact by clinical translation to perform alpha particle radiation therapy with ^{211}At.

What was the impact on society beyond science and technology?
If there is nothing significant to report during this reporting period, state "Nothing to Report."

Describe how results from the project made an impact, or are likely to make an impact, beyond the bounds of science, engineering, and the academic world on areas such as:

- *improving public knowledge, attitudes, skills, and abilities;*
- *changing behavior, practices, decision making, policies (including regulatory policies), or social actions; or*
- *improving social, economic, civic, or environmental conditions.*

Results from this project could make an impact on society by improving public knowledge about cancer therapy. The targeted alpha particle radiation therapy is an emerging technology to improve cancer treatment efficacy.

5. CHANGES/PROBLEMS: *The PD/PI is reminded that the recipient organization is required to obtain prior written approval from the awarding agency grants official whenever there are significant changes in the project or its direction. If not previously reported in writing, provide the following additional information or state, "Nothing to Report," if applicable:*

Changes in approach and reasons for change
Describe any changes in approach during the reporting period and reasons for these changes. Remember that significant changes in objectives and scope require prior approval of the agency.

Nothing to report.

Actual or anticipated problems or delays and actions or plans to resolve them
Describe problems or delays encountered during the reporting period and actions or plans to resolve them.

Due to the COVID-19 pandemic, the research progress was delayed. We received a one-year extension to finish this project.

Changes that had a significant impact on expenditures
Describe changes during the reporting period that may have had a significant impact on expenditures, for example, delays in hiring staff or favorable developments that enable meeting objectives at less cost than anticipated.

Nothing to report.

Significant changes in use or care of human subjects, vertebrate animals, biohazards, and/or select agents
Describe significant deviations, unexpected outcomes, or changes in approved protocols for the use or care of human subjects, vertebrate animals, biohazards, and/or select agents during the reporting period. If required, were these changes approved by the applicable institution committee (or equivalent) and reported to the agency? Also specify the applicable Institutional Review Board/Institutional Animal Care and Use Committee approval dates.

Significant changes in use or care of human subjects

Human subjects are not involved in this project.

Significant changes in use or care of vertebrate animals

There are no significant changes in use or care of vertebrate animals.

Significant changes in use of biohazards and/or select agents

There are no significant changes in use of biohazards or select agents.

6. **PRODUCTS:** *List any products resulting from the project during the reporting period. If there is nothing to report under a particular item, state "Nothing to Report."*

- **Publications, conference papers, and presentations**
  Report only the major publication(s) resulting from the work under this award.

  Journal publications. *List peer-reviewed articles or papers appearing in scientific, technical, or professional journals. Identify for each publication: Author(s); title; journal; volume: year; page numbers; status of publication (published; accepted, awaiting publication; submitted, under review; other); acknowledgement of federal support (yes/no).*

We have one paper accepted for publication in the International Journal of Nanomedicine. The federal support is acknowledged. Yang Liu, Zhengyuan Zhou, Yutian Feng, Xiao-Guang Zhao, Ganesan Vaidyanathan, Michael R. Zalutsky, Tuan Vo-Dinh. Gold nanostars: A novel platform for developing ^{211}At-labeled agents for targeted alpha-particle therapy. Accepted. The federal support is acknowledged in this journal publication.

  Books or other non-periodical, one-time publications. *Report any book, monograph, dissertation, abstract, or the like published as or in a separate publication, rather than a periodical or series. Include any significant publication in the proceedings of a one-time conference or in the report of a one-time study, commission, or the like. Identify for each one-time publication: author(s); title; editor; title of collection, if applicable; bibliographic information; year; type of publication (e.g., book, thesis or dissertation); status of publication (published; accepted, awaiting publication; submitted, under review; other); acknowledgement of federal support (yes/no).*

We submitted an abstract to the conference Pacifichem 2021 and the abstract has been accepted for oral presentation. The federal support is acknowledged. Yang Liu, Zhengyuan Zhou, Ganesan Vaidyanathan, Michael R. Zalutsky, Tuan Vo-Dinh. Gold nanoparticles as a novel delivery strategy for targeted alpha therapy. Accepted.

  Other publications, conference papers and presentations. *Identify any other publications, conference papers and/or presentations not reported above. Specify the status of the publication as noted above. List presentations made during the last year (international, national, local societies, military meetings, etc.). Use an asterisk (*) if presentation produced a manuscript.*

Nothing to report.

- **Website(s) or other Internet site(s)**
  List the URL for any Internet site(s) that disseminates the results of the research activities. A short description of each site should be provided. It is not necessary to include the publications already specified above in this section.

Nothing to report.

- **Technologies or techniques**
  Identify technologies or techniques that resulted from the research activities. Describe the technologies or techniques were shared.

From this project, we developed gold nanoparticles as a novel delivery strategy for targeted alpha particle therapy to treat cancer. The developed technology was shared by publishing a peer-reviewed paper in the International Journal of Nanomedicine. In addition, I shared the developed technology by giving an oral presentation in the conference Pacifichem 2021.

- **Inventions, patent applications, and/or licenses**
  Identify inventions, patent applications with date, and/or licenses that have resulted from the research. Submission of this information as part of an interim research performance progress report is not a substitute for any other invention reporting required under the terms and conditions of an award.

Nothing to report.

- **Other Products**
  Identify any other reportable outcomes that were developed under this project. Reportable outcomes are defined as a research result that is or relates to a product, scientific advance, or research tool that makes a meaningful contribution toward the understanding, prevention, diagnosis, prognosis, treatment and /or rehabilitation of a disease, injury or condition, or to improve the quality of life. Examples include:
  - *data or databases;*
  - *physical collections;*
  - *audio or video products;*
  - *software;*
  - *models;*
  - *educational aids or curricula;*
  - *instruments or equipment;*
  - *research material (e.g., Germplasm; cell lines, DNA probes, animal models);*
  - *clinical interventions;*
  - *new business creation; and*
  - *other.*

Nothing to report.

7. PARTICIPANTS & OTHER COLLABORATING ORGANIZATIONS

What individuals have worked on the project?
Provide the following information for: (1) PDs/PIs; and (2) each person who has worked at least one person month per year on the project during the reporting period, regardless of the source of compensation (a person month equals approximately 160 hours of effort). If information is unchanged from a previous submission, provide the name only and indicate "no change".

Example:

Name:	*Mary Smith*
Project Role:	*Graduate Student*
Researcher Identifier (e.g. ORCID ID):	*1234567*
Nearest person month worked:	*5*
Contribution to Project:	*Ms. Smith has performed work in the area of combined error-control and constrained coding.*
Funding Support:	*The Ford Foundation (Complete only if the funding support is provided from other than this award.)*

Name: Yang Liu
Project Role: Principal Investigator
Researcher Identifier (ORCID ID): 0000-0003-3640-8852
Nearest person month worked: 27
Contribution to Project: Yang Liu is the PI for this project and has been actively involved in the whole project including targeted nanoparticles development, radiolabeling test, in vitro, and in vivo studies.

Has there been a change in the active other support of the PD/PI(s) or senior/key personnel since the last reporting period?
If there is nothing significant to report during this reporting period, state "Nothing to Report."

If the active support has changed for the PD/PI(s) or senior/key personnel, then describe what the change has been. Changes may occur, for example, if a previously active grant has closed and/or if a previously pending grant is now active. Annotate this information so it is clear what has changed from the previous submission. Submission of other support information is not necessary for pending changes or for changes in the level of effort for active support reported previously. The awarding agency may require prior written approval if a change in active other support significantly impacts the effort on the project that is the subject of the project report.

Nothing to report.

What other organizations were involved as partners?
If there is nothing significant to report during this reporting period, state "Nothing to Report."

Describe partner organizations – academic institutions, other nonprofits, industrial or commercial firms, state or local governments, schools or school systems, or other organizations (foreign or domestic) – that were involved with the project. Partner organizations may have provided financial or in-kind support, supplied facilities or equipment, collaborated in the research, exchanged personnel, or otherwise contributed.

Provide the following information for each partnership:
Organization Name:
Location of Organization: (if foreign location list country)
Partner's contribution to the project (identify one or more)

- *Financial support;*
- *In-kind support (e.g., partner makes software, computers, equipment, etc., available to project staff);*
- *Facilities (e.g., project staff use the partner's facilities for project activities);*
- *Collaboration (e.g., partner's staff work with project staff on the project);*
- *Personnel exchanges (e.g., project staff and/or partner's staff use each other's facilities, work at each other's site); and*
- *Other.*

Nothing to report.

8. SPECIAL REPORTING REQUIREMENTS

Generic Award Chart:

W81XWH1910684: Targeted Gold Nanoparticles (AuNPs) for Potent Alpha-Particle Radiotherapy of Brain Cancer

PI: Yang Liu, Duke University, NC **Budget:** $240,041.00

Topic Area: FY 2018 DoD PRCRP, Horizon Award **Mechanism:** W81XWH-18-PRCRP-HA

Research Area(s): 0805, 0808, 0817 **Award Status:** 15-Aug-2019 To 14-Feb-2022

Study Goals:

The overall objective of this research is to develop a novel image-guided ^{211}At radiotherapy with targeted AuNPs for aggressive brain cancer treatment.

Specific Aims:

1. Synthesize, optimize and evaluate targeted AuNPs for ^{211}At and ^{124}I labeling.
2. Conjugate AuNPs with tumor-homing peptides for brain cancer targeting and perform in vitro tests to demonstrate the developed nanoagent can target and treat brain cancer.
3. Evaluate in vivo brain cancer uptake, biodistribution, pharmacokinetics, and therapeutic effect of targeted AuNPs with both ^{211}At and ^{124}I labeling using a murine animal model.

Key Accomplishments and Outcomes:

Publications: 1
Patents: none to date
Funding Obtained: none to date

9. APPENDICES: *Attach all appendices that contain information that supplements, clarifies or supports the text. Examples include original copies of journal articles, reprints of manuscripts and abstracts, a curriculum vitae, patent applications, study questionnaires, and surveys, etc.*

A copy of my published paper and conference abstract are in the attachment.

International Journal of Nanomedicine

Dovepress
open access to scientific and medical research

Open Access Full Text Article

ORIGINAL RESEARCH

Gold Nanostars: A Novel Platform for Developing ^{211}At-Labeled Agents for Targeted Alpha-Particle Therapy

International Journal of Nanomedicine downloaded from https://www.dovepress.com/ on 05-Mar-2022
For personal use only.

Yang Liu[1]
Zhengyuan Zhou[2]
Yutian Feng[2]
Xiao-Guang Zhao[2]
Ganesan Vaidyanathan[2]
Michael R Zalutsky[1,2]
Tuan Vo-Dinh[1,3,4]

[1]Department of Biomedical Engineering, Duke University, Durham, NC, 27708, USA; [2]Department of Radiology, Duke University Medical Center, Durham, NC, 27710, USA; [3]Department of Chemistry, Duke University, Durham, NC, 27708, USA; [4]Fitzpatrick Institute for Photonics, Duke University, Durham, NC, 27708, USA

Aim: To develop an innovative ^{211}At nanoplatform with high radiolabeling efficiency and low in vivo deastatination for future targeted alpha-particle therapy (TAT) to treat cancer.

Methods: Star-shaped gold nanoparticles, gold nanostars (GNS), were used as the platform for ^{211}At radiolabeling. Radiolabeling efficiency under different reaction conditions was tested. Uptake in the thyroid and stomach after systemic administration was used to evaluate the in vivo stability of ^{211}At-labeled GNS. A subcutaneous U87MG human glioma xenograft murine model was used to preliminarily evaluate the therapeutic efficacy of ^{211}At-labeled GNS after intratumoral administration.

Results: The efficiency of labeling GNS with ^{211}At was almost 100% using a simple and rapid synthesis process that was completed in only 1 min. In vitro stability test in serum showed that more than 99% of the ^{211}At activity remained on the GNS after 24 h incubation at 37°C. In vivo biodistribution results showed low uptake in the thyroid (0.44–0.64%ID) and stomach (0.21–0.49%ID) between 0.5 and 21 h after intravenous injection, thus indicating excellent in vivo stability of ^{211}At-labeled GNS. The preliminary therapeutic efficacy study demonstrated that ^{211}At labeled GNS substantially reduced tumor growth ($P < 0.001$; two-way ANOVA) after intratumoral administration.

Conclusion: The new ^{211}At radiolabeling strategy based on GNS has the advantages of a simple process, high labeling efficiency, and minimal in vivo dissociation, making it an attractive potential platform for developing TAT agents that warrants further evaluation in future preclinical studies directed to evaluating prospects for clinical translation.

Keywords: astatine-211, ^{211}At, gold nanostars, GNS, cancer therapy, targeted alpha-particle therapy, TAT

Introduction

Targeted alpha-particle therapy (TAT) is an emerging method for cancer treatment that has the advantages of high linear energy transfer (>50 keV/μm), irreparable double-strand DNA breaks, and independence of dose rate, cell cycle, and cellular oxygenation.[1,2] As a result, TAT is conceptually superior to standard-of-care external beam radiation therapy using X-rays or γ-rays particularly for treating hypoxic tumors. Furthermore, since alpha-particles have a range of only a few cell diameters, TAT is an attractive approach for treating disseminated cancers.[3] Among the different available alpha-particle emitting radionuclides, astatine-211 (^{211}At) has the unique advantages of an optimal half-life (7.2 h) and absence of long-lived alpha-particle emitting daughter radionuclides, thus preventing off-target radiation toxicity from the

Correspondence: Michael R Zalutsky
Department of Radiology, Duke University Medical Center, 311 Research Drive, 161H Bryan Research Building, Durham, NC, 27710, USA
Email michael.zalutsky@duke.edu

Tuan Vo-Dinh
Department of Biomedical Engineering, Duke University, 1427 CIEMAS, Box 90281, Durham, NC, 27708, USA
Tel +1 919 660-8520
Email tuan.vodinh@duke.edu

Received: 2 July 2021
Accepted: 28 August 2021
Published: 28 October 2021

© 2021 Liu et al. This work is published and licensed by Dove Medical Press Limited. The full terms of this license are available at https://www.dovepress.com/terms.php and incorporate the Creative Commons Attribution – Non Commercial (unported, v3.0) License (http://creativecommons.org/licenses/by-nc/3.0/). By accessing the work you hereby accept the Terms. Non-commercial uses of the work are permitted without any further permission from Dove Medical Press Limited, provided the work is properly attributed. For permission for commercial use of this work, please see paragraphs 4.2 and 5 of our Terms (https://www.dovepress.com/terms.php).

redistribution of daughter radionuclides.[2,4] Our group performed the first clinical trial for the treatment of glioblastoma (GBM) with ^{211}At-labeled antibodies.[5] However, traditional ^{211}At radiolabeling methods including the one used in this clinical study generate a chemical bond between ^{211}At and an aromatic carbon that have the following limitations: (1) the complicated radiochemistry process makes it difficult for clinical applications; (2) low conjugation efficiency results could lead to suboptimal cancer treatment: only 1 in 400 to 1000 antibody molecules can be labeled with an ^{211}At; (3) the ^{211}At from the labeled molecule can dissociate from the prosthetic moiety due to intrinsic low C-At bond strength and in vivo metabolic degradation.[6,7] Innovative radiolabeling methods involving a simple process, high yield, and loading capacity are urgently needed for both preclinical studies and clinical translation of TAT agents labeled with ^{211}At.

Our group has developed a novel method to synthesize star-shaped gold nanoparticles, gold nanostars (GNS), for biomedical applications without the need for toxic surfactants.[8] The multibranched GNS morphology offered a high surface area for ^{211}At labeling, which helped achieve a very effective delivery platform. Furthermore, the size of GNS can be tailored to optimize the preferential accumulation in tumors by the enhanced permeability and retention effect. In prior studies, we have demonstrated that the developed GNS can accumulate selectively in brain cancer mediated by the enhanced permeability and retention effect.[9] The enhanced permeability and retention effect was reported to be due to the tumor leaky vasculature, and this effect was found in most solid tumors.[10,11] Brain cancer was selected as the intended target disease for this study because it is one of the most aggressive cancers. Specifically, GBM, with more than 10,000 newly diagnosed patients in the United States each year, is the most common primary brain cancer.[12,13] Despite the highest first-year cost (> $120,000) for a cancer type, the prognosis for GBM patients is dismal. The median survival for GBM patients is only 15 months after aggressive treatments, including surgery, chemotherapy, and radiation therapy.[14–16] Less than 5% of the patients survive for more than 3 years.[17] Despite decades of effort, GBM is still a deadly disease with essentially 100% mortality.[18,19] Thus, there is a critical and urgent need to develop new approaches for effective brain cancer treatment.

As a first step towards developing a GNS-based ^{211}At-labeled TAT agent for GBM treatment, we have performed experiments described herein evaluating the potential utility of ^{211}At-labeled GNS for this purpose. Only a few studies have been reported directed at developing nanoparticle-driven carrier systems for use with ^{211}At. Ultrashort, single-walled carbon nanotubes (US-tubes) labeled with ^{211}At via noncovalent van der Waals binding have been evaluated in an ex vivo study.[20] However, the radiolabeling efficiency was low, and the in vivo stability of ^{211}At-labeled US-tubes was not studied. Although in vitro cell experiments have been performed with ^{211}At-labeled gold nanospheres, no in vivo investigations of gold nanoparticles have been described to date.[21,22]

In the current study, we evaluated GNS as a novel platform technology for ^{211}At radiolabeling and for the first time, investigated in vivo stability and biodistribution in normal mice, and therapeutic efficacy of the ^{211}At-GNS in a murine subcutaneous GBM model. Our experimental results showed that ^{211}At labeling of GNS can be achieved by a simple process in a short time with a high labeling efficiency and in vivo stability. In addition, the ^{211}At-labeled GNS demonstrated a substantial therapeutic efficacy by inhibiting tumor growth after intratumoral administration. To the best of our knowledge, this is the first in vivo study investigating gold nanoparticles as an ^{211}At delivery platform for future TAT applications.

Materials and Methods

GNS Synthesis and Characterization

All chemicals were purchased from Sigma-Aldrich unless mentioned otherwise. GNS were synthesized following our developed toxic surfactant-free and seed-mediated method reported in previous studies.[23,24] 12-nm spherical gold nanoparticles synthesized using the trisodium citrate reduction method were used as seeds. For GNS synthesis, 1 mL of 3 mM $AgNO_3$ in deionized (DI) water and 1 mL of 50 mM ascorbic acid in DI water were rapidly added to a mixture of 100 mL of DI water with 0.25 mM $HAuCl_4$, 1 mM HCl, and 1 mL of the 12-nm gold nanosphere seeds under vigorous stirring. After a 10-min reaction, 1 mL of 1 mM mPEG-SH (MW 6,000) in DI water was added and the mixture was incubated for 1 h at room temperature. The resultant GNS were purified and concentrated by centrifugation at 6000 g for 30 min. Transmission electron microscopy (TEM) of GNS was performed using a Tecnai G^2 Twin transmission electron microscope (FEI, Hillsboro, OR) with a 160 kV acceleration voltage. The Vis-NIR spectrum was obtained by using a UV-Vis-NIR spectrometer (UV-3600, Shimadzu, Japan). The hydrodynamic

diameter and nanoparticle concentration of the PEGylated GNS were measured with Nanoparticle Tracking Analysis method (Nanosight 500, Malvern, UK).

Radiolabeling and in vitro Stability

Astatine-211 was produced at the Duke University Medical Center cyclotron facility by bombarding a natural bismuth target with a 28.0-MeV alpha-particle beam and subsequently isolated by a dry distillation method.[25] For the radiolabeling experiments, 100 μg GNS in DI water were mixed with 7.4 MBq ^{211}At (460 fmol) in different media [DI water, 0.1 M NaOH in DI water, 50 mM ascorbic acid (AA) in DI water, or 0.2 mg/mL N-chlorosuccinimide (NCS) in DI water], and the reaction was allowed to proceed at room temperature for 1, 5 and 30 min. We also evaluated the effect of the GNS amount – ranging from 100 μg (540 fmol) down to 0.01 μg (54 amol) – on radiolabeling efficiency using a 5-min reaction time. The reaction volume was 100 μL, and centrifugation (6,000 g, 10 min) was used to separate free, unreacted ^{211}At remaining in solution and ^{211}At-labeled GNS. The ^{211}At-labeled GNS pellet was resuspended in 100 μL of DI water, and then the radioactivity levels were measured using a dose calibrator. The stability of ^{211}At-labeled GNS was evaluated by incubating it in phosphate-buffered saline (PBS), pH 7.4, and in murine serum at 37°C up to 24 h. The murine serum was isolated by centrifugating the murine whole blood at 3000 g for 10 min. The supernatant (serum) was collected for the in vitro stability measurements. The concentration of the ^{211}At-GNS agent in both the murine serum and PBS was 200 μg/mL (Au) with 7.4 MBq ^{211}At per mL. The same centrifugation protocol (6,000 g, 10 min) was used to separate dissociated ^{211}At in the solution and the ^{211}At-labeled GNS.

In vivo Biodistribution

Freshly prepared PEGylated GNS were labeled with ^{211}At by incubation at room temperature for 5 min in 50 mM ascorbic acid in DI water. Radiolabeled GNS were purified by centrifugation/washing 3 times and resuspended in PBS without ascorbic acid. For the biodistribution experiment, 20 nude mice were randomly divided into 4 groups, and each mouse was intravenously injected with ^{211}At-labeled GNS (0.185 MBq radioactivity and 100 μg gold mass) in 100 μL PBS without ascorbic acid. Mice were euthanized, and organs of interest (liver, spleen, lung, heart, kidney, bladder, stomach, small intestine, large intestine, thyroid, muscle, blood, urine, bone, skin, brain, and tail) were harvested at 0.5, 2, 14, and 21 h after intravenous injection of the radiolabeled GNS. Tissues were weighed and counted along with injection standards for ^{211}At activity using an automated gamma counter (LKB 1282, Wallac, Finland). The measurement geometry of the gamma counter was taken into account by placing samples at the same location as that for the standard. From these counts, the percent injected dose per gram tissue (%ID/g) and percent injected dose per organ (%ID/organ) were calculated using an in-house computer program.

Therapeutic Efficacy Experiment

Human glioma U87MG cells were obtained from Duke Cell Culture Facility and cultured in MEM cell growth medium with 10% fetal bovine serum (Hyclone, MA, USA), 100 units/mL penicillin, and 100 μg/mL streptomycin at 37°C in a 5% CO_2 incubator. The use of the U87MG cell line was approved by the ethics committee, and this cell line was authenticated by the short tandem repeat profiling. All animal studies were performed under protocols that had been approved by the Duke University Institutional Animal Care and Use Committee. The guidelines from National Institutes of Health and Duke University Institutional Animal Care and Use Committee were followed. For subcutaneous xenograft generation, 3×10^6 U87MG human glioma cells in the cell growth medium were subcutaneously injected into each mouse in the flank region. The tumor size was calculated as 0.5×length×width×width. After 18 days, the tumor size reached ~100 mm^3 and the intratumoral therapy study was initiated. Groups of 10 mice received either 30 μL of ^{211}At-labeled GNS (1.11 MBq) in PBS or just PBS by intratumoral injection using a syringe pump at a rate of 30 μL/min. The tumor sizes were measured every 3 or 4 days until the end of the study.

Results

The synthesized GNS exhibited a star-like shape and had a maximum absorption at 765 nm (Figure 1). We performed ^{211}At radiolabeling experiments using PEGylated GNS with a hydrodynamic diameter of 50 nm using different reaction conditions and the results are shown in Figure 2. First, we compared the radiolabeling efficiency in four different reaction media. The calculated ^{211}At labeling efficiency was 94.7 ± 0.1% in DI water, 97.4 ± 0.2% in DI water with 0.1 M NaOH, 99.8 ± 0.1% in DI water with 50 mM ascorbic acid, and 42.6 ± 0.3% in DI

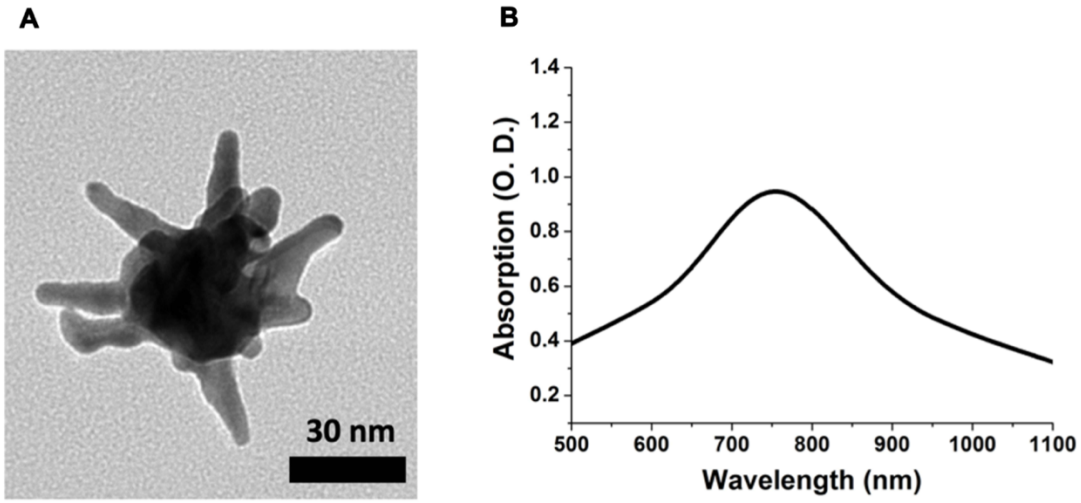

Figure 1 TEM image (**A**) and Vis-NIR absorption spectrum (**B**) of the synthesized GNS used in this study.

water with 0.2 mg/mL NCS. The radiolabeling efficiency for the reaction medium with a reducing agent, ascorbic acid, was the highest (99.8%), and almost all the ^{211}At could be attached to GNS after only a 5-min incubation at room temperature. Conversely, the NCS oxidizing agent dramatically decreased the radiolabeling efficiency to 42.6 ± 0.3%. Second, we evaluated the effect of incubation time on radiolabeling efficiency in reaction media consisting of DI water or DI water with 50 mM ascorbic acid. The radiolabeling efficiency in DI water increased from 93.4 ± 0.2% (1 min), to 94.7 ± 0.1% (5 min), and 97.4 ± 0.2% (30 min). The radiolabeling efficiency in DI water with 50 mM ascorbic acid was essentially quantitative by 1 min and remained constant over 30 min. Third, we compared how the nanoparticle-to-^{211}At ratio affected the radiolabeling using DI water with 50 mM ascorbic acid as the reaction medium. The radiolabeling efficiency decreased as the ^{211}At:GNS ratio increased: from 99.8 ± 0.1% (540 fmol GNS, ^{211}At:GNS = 0.85), 99.1 ± 0.1% (54 fmol GNS, ^{211}At:GNS = 8.5), 98.3 ± 0.1% (5.4 fmol GNS, ^{211}At:GNS = 85), 94.1 ± 0.2% (540 amol GNS, ^{211}At:GNS = 850), and 67.4 ± 0.2% (54 amol GNS, ^{211}At:GNS = 8,500). The in vitro stability tests at 37°C indicated that 99.5 ± 0.3% and 99.6 ± 0.2% ^{211}At remained on GNS after 1 h incubation in PBS and serum, respectively. After 24 h incubation, the percentage of ^{211}At on GNS was 98.9 ± 0.2% for PBS and 99.1 ± 0.3% for serum at 37°C.

After evaluating the feasibility of labeling GNS with ^{211}At, we performed a comprehensive study to investigate the biodistribution of ^{211}At activity in normal mice after intravenous injection of ^{211}At-labeled GNS. As shown in Figure 3, at 30 min, blood was found to have the highest concentration of ^{211}At activity (44.4 ± 4.5%ID/g) followed by spleen (22.6 ± 1.8%ID/g), lungs (16.9 ± 2.0%ID/g), liver (9.1 ± 2.2%ID/g) and kidneys (8.1 ± 1.1%ID/g). In total, nearly 60%ID was found in the blood pool and ~13% ID was found in the liver. Activity in the blood decreased with time between 0.5 and 21 h after intravenous injection – from 44.4 ± 4.5%ID/g at 0.5 h to 40.6 ± 3.2%ID/g, 22.9 ± 4.17%ID/g and 22.0 ± 4.7%ID/g remaining at 2, 14 and 21 h, respectively. Similar behavior was observed in the lungs. In contrast, the %ID/g in spleen increased with time, from 22.6 ± 1.9%ID/g at 0.5 h, to 37.5 ± 5.9%ID/g at 2 h, 35.3 ± 4.7%ID/g at 14 h, and 105.3 ± 15.8%ID/g at 21 h; a similar trend was observed in the liver. For radiohalogens like ^{211}At, uptake in the thyroid and the stomach can serve as an indicator of in vivo stability because of the proclivity of free halides for these tissues. The %ID in thyroid was low and did not change significantly between 0.5 and 21 h, with values of 0.61 ± 0.21%ID, 0.64 ± 0.28% ID, 0.44 ± 0.18%ID, and 0.61 ± 0.21%ID measured at 0.5, 2, 14 and 21 h, respectively. Likewise, the %ID in the stomach was low at all time points: 0.21 ± 0.06%ID at 0.5h, 0.28 ± 0.08%ID at 2h, 0.43 ± 0.14%ID at 14 h, and 0.49 ± 0.10%ID at 21 h. In summary, the biodistribution

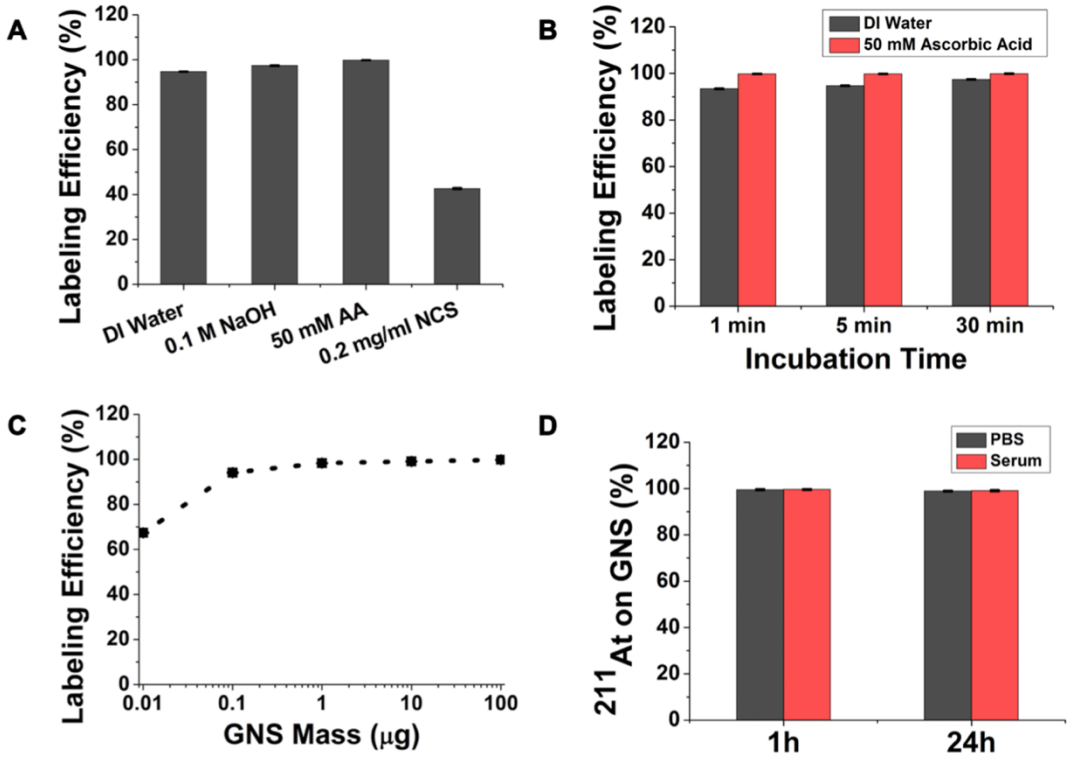

Figure 2 Evaluation of radiolabeling GNS with ^{211}At. (**A**). Radiolabeling efficiency evaluation in different reaction media: DI water, DI water with 0.1 M NaOH, DI water with 50 mM ascorbic acid, DI water with 0.2 mg/mL NCS after a 5 min incubation. (**B**) Radiolabeling efficiency as a function of incubation time when the reaction was performed using DI water or DI water with 50 mM ascorbic acid as the media. (**C**) Radiolabeling efficiency evaluation for GNS mass ranging from 0.01–100 μg for 5 min incubation in DI water with 50 mM ascorbic acid. (**D**) Percentage of ^{211}At remaining on GNS after incubation in PBS and murine serum at 37°C for 1 h and 24 h. All experiments performed in triplicate and error bar shows standard deviation.

results showed that ^{211}At-labeled GNS had a long circulation time in the blood and accumulated in the liver and spleen gradually, with a low degree of deastatination in vivo.

As an initial evaluation of the therapeutic potential of ^{211}At-labeled GNS, an experiment was performed in athymic mice with subcutaneous U87MG human glioma xenografts with the labeled drug given by the intratumoral route. As shown in Figure 4, the ^{211}At-labeled GNS substantially inhibited the tumor growth rate. The average tumor volume in the control group increased rapidly from 82 mm^3 on Day 1 to 177 mm^3, 409 mm^3, 798 mm^3, and 1456 mm^3 on Days 4, 7, 10, and 14, respectively. In contrast, the average tumor volume in the treatment group increased slowly, from 78 mm^3 on Day 1 to 95 mm^3, 112 mm^3, 152 mm^3, and 189 mm^3 on Days 4, 7, 10, and 14, respectively. The two-way ANOVA test indicated that the difference in tumor volumes between the ^{211}At-labeled GNS treated group and the control group with PBS injection was statistically significant ($P < 0.001$).

Discussion

The multibranched GNS morphology of GNS offered a high surface area for loading ^{211}At, which should provide a very effective delivery platform. Consistent with this expectation, our developed GNS had a very promising performance as a nanoplatform for ^{211}At delivery. First, the radiolabeling process is simple and can be completed as fast as 1 min with nearly quantitative labeling efficiency (99.8%). Moreover, the radiolabeling process can be performed without using the organic solvents or a high-performance liquid chromatography system for purification as is generally required for traditional radiolabeling methods based on At-C chemical bond formation. Second, the GNS loading capacity for ^{211}At is high and the radiolabeling efficiency remained at ~94% when an ^{211}At:GNS ratio

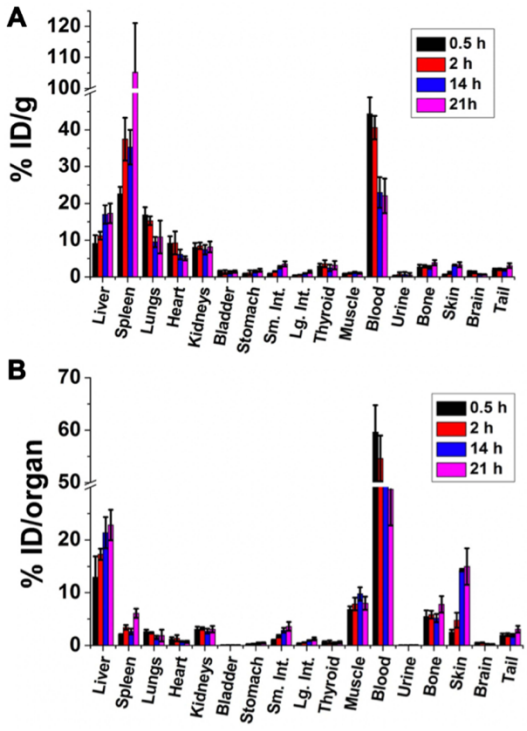

Figure 3 Biodistribution of ^{211}At activity after intravenous injection of ^{211}At-labeled GNS in normal mice. The results are shown as percent injected dose per gram tissue (%ID/g) (**A**), and as percent injected dose per organ (%ID/organ) (**B**). Error bar shows the standard deviation (n=5).

of 850 was used. The radiolabeling efficiency dropped to 67.4% when we further increased the ^{211}At:GNS ratio to 8,500, indicating that the maximum number of ^{211}At loaded per GNS was approximately 5,700. In contrast, traditional macromolecular radiolabeling methods based on At-C chemical bond formation generally have a low conjugation efficiency: only 1 in 400 to 1,000 antibody molecules can be labeled with an ^{211}At radionuclide.[2] Third, the ^{211}At-labeled GNS exhibited high stability and minimal in vivo dissociation. The thyroid and stomach are the two major organs that take up high amounts of free [^{211}At] astatide. We observed a low uptake of ^{211}At activity in the thyroid (0.44–0.61%ID) and the stomach (0.21–0.49%ID) between 0.5 h and 21 h after systemic administration of ^{211}At-labeled GNS, suggesting a low degree of in vivo dehalogenation had occurred.

The observed high in vivo stability of ^{211}At labeled GNS can be explained by the strong chemical bond formed between At and Au.[26] The calculated bond energy was reported to be 130 kJ/mol and the oxidation state for ^{211}At for binding to Au was considered to be −1.[26] Our radiolabeling results are consistent with this; in the presence of a reducing agent, ascorbic acid, ^{211}At labeling of GNS increased, while in the presence of an oxidizing agent, NCS, ^{211}At labeling of GNS decreased, indicating that the oxidization state of At on GNS is −1. We plan to perform mechanistic studies to better understand our

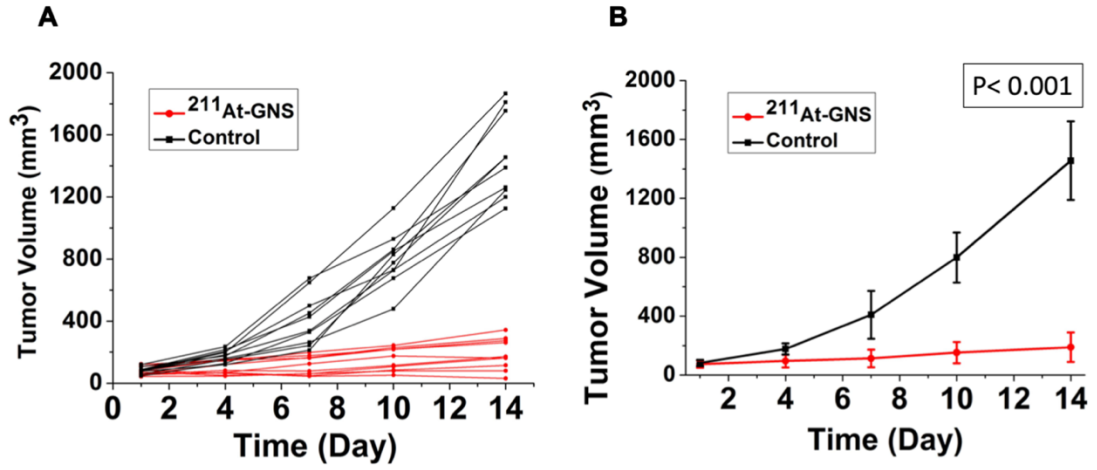

Figure 4 Therapeutic efficacy evaluation of ^{211}At TAT using GNS as a novel delivery platform. (**A**) tumor size change profile for each mouse in the ^{211}At-GNS treatment group (1.11 MBq) and blank control group with PBS injection. (**B**) Average tumor size change profile for mice in the ^{211}At-GNS treatment group (1.11 MBq) and blank control group with PBS injection. Error bar shows standard deviation (n = 10). P value was calculated using 2-way ANOVA (P< 0.001).

in vivo experimental data in the near future using approaches similar to those used by Teze et al.[6]

The in vivo stability of the ^{211}At-labeled TAT agent is critical because dissociated ^{211}At can result in off-targeted toxicity and decrease the radiation dose delivered to the tumor. To provide a frame of reference, we compared our in vivo stability results with those from previous studies in mice using clinically applied ^{211}At coupling reagents including N-succinimidyl 3-trimethylstannylbenzoate (m-MeATE) and isothiocyantophenethyl-ureido-closodecaborate(2-) (B10-NCS). Using a murine model, Zalutsky et al reported the stomach uptake for an ^{211}At-labeled antibody prepared using m-MeATE to be 2.94–4.07%ID/g between 0.5 and 24 h after IV injection with a thyroid uptake of 0.36–0.73%ID.[27] In a separate biodistribution study using the same m-MeATE reagent for labeling an antibody F(ab')$_2$ fragment with ^{211}At, Bäck et al reported that the stomach uptake was 4.4–12.3% ID/g during 0.5–21 h after IV injection,[28] which is significantly higher than that (0.71–1.79%ID/g) for our GNS delivery platform. Orozco et al utilized the B10-NCS coupling reagent to label an anti-CD45 antibody with ^{211}At and reported a stomach uptake of 1–2%ID/g between 1 h and 7 h, reaching ~5%ID/g at 24 h.[29]

We next compared our in vivo stability results with those for other ^{211}At TAT agents moving toward clinical trial including meta-[^{211}At]astatobenzylguanidine (^{211}At-MABG), and N-succinimidyl 3-((1,2-bis(tert-butoxycarbonyl)guanidino) methyl)-5-(trimethylstannyl)benzoate (Boc_2-iso-SGMTB). Ohshima et al reported that for ^{211}At-MABG, stomach uptake was 2.41–6.71%ID/g and thyroid uptake was 0.61–1.65%ID between 1 and 24 h after injection.[30] Choi et al utilized the Boc_2-iso-SGMTB linker to label a single-domain antibody fragment (sdAb) with ^{211}At and reported a stomach uptake of 0.5–1.7%ID/g and thyroid uptake of 0.15–0.35%ID over up to 24 h after injection.[7] In addition, there are some other ^{211}At-coupling reagents at earlier stages of development that provide data for comparison. For example, Dekempaner evaluated the N-[2-(maleimido)ethyl]-3-(trimethylstannyl) benzamide (MSB) coupling reagent in comparison to Boc_2-SGMTB, m-MeATE for labeling an sdAb with ^{211}At.[31] The reported stomach uptake for ^{211}At-labeled sdAb using MSB was more than 20%ID/g between 1 and 6 h after injection. Better in vivo stability was observed with sdAb labeled using m-MeATE, but stomach uptake was still more than 10%ID/g even at 1 h after injection. Consistent with the results of Choi et al,[7] ^{211}At-labeled sdAb prepared using Boc_2-SGMTB had the lowest stomach uptake among the three studied methods, with ~2%ID/g between 1 and 6 h after injection.

With regard to the in vivo stability of small organic molecule TAT agents labeled with ^{211}At, Ohshima reported that for [^{211}At]astatophenylalanine, stomach uptake was 0.6–2.99%ID/g during the first 6 h after injection.[32] Makvandi et al evaluated the in vivo stability of [^{211}At] MM4 (1-(4-astatophenyl)-8,9-dihydro-2,7,9atriazabenzo [cd]azulen-6(7H)-one) and stomach uptake was more than 10%ID/g within 2 h after injection.[33] Liu et al radiolabeled a small-molecule peptide with ^{211}At by using an N-succinimidyl 5-(tributylstannyl)-3-pyridinecarboxylate ester precursor and reported the stomach uptake to be 5.55%ID/g 3 h after intravenous injection.[34] However, in a subsequent therapy study using this molecule, gastric toxicity was observed at higher doses.[35] In summary, although different animal models were used, uptake of ^{211}At activity in the stomach and thyroid after injection of ^{211}At-labeled GNS is lower than that observed for most other ^{211}At-labeled TAT agents, including those that have either been investigated clinically or will soon enter clinical trials. This suggests that the GNS delivery platform has sufficient in vivo stability for future clinical translation.

It is worth noting that GNS have other properties that may provide advantages compared with more conventional gold nanoparticle configurations, particularly when combination therapeutic strategies are contemplated. GNS have tip-enhanced plasmonics with a dramatically increased electromagnetic field near the sharp tip, making them a superior nanoplatform for certain imaging and therapy approaches. For example, we have used GNS for in vivo surface-enhanced Raman spectroscopy for cancer detection in a sarcoma murine animal model.[36] In addition, we have used GNS for both in vitro and in vivo high-resolution imaging with two-photon photoluminescence. The GNS have an extremely high two-photon cross section, which is up to 4 orders of magnitude higher than that for gold nanospheres.[37] As a result, we can image a single GNS under two-photon photoluminescence imaging.[38] The GNS capability for sensitive optical imaging at the subcellular level makes it an attractive theranostic platform for image-guided therapy and to investigate the therapeutic efficacy of TAT with ^{211}At. We have also used GNS for photothermal therapy and our experimental results demonstrated that GNS are superior to gold nanoshells, which are under clinical trial to treat prostate cancer with photothermal therapy.[39] Therefore, GNS are an

attractive nanoplatform because they can be used for combining photothermal therapy and TAT with the aim of generating synergistically effective cancer treatments.

A preliminary therapeutic efficacy study on a human GBM flank tumor murine model demonstrated that TAT therapy with ^{211}At-labeled GNS can dramatically decrease tumor growth. With a high linear energy transfer, TAT therapy can generate irreparable DNA double-strand breaks with a therapeutic effect that is independent of tissue oxygen level, which is superior to traditional external beam radiation therapy. External beam radiation therapy is characterized as a low linear energy transfer, reparable DNA single-strand break generating radiation, with the requirement of oxygen to generate radical oxygen species for therapeutic effect. In previous studies, we radiolabeled these same GNS with ^{124}I and performed PET/CT imaging in mice with intracranial tumors and demonstrated that the GNS could accumulate selectively in brain tumors with tumor-to-normal ratios of up to 7.8:1.[9] In future studies, we plan to use a similar intracranial GBM murine animal model to evaluate the therapeutic efficacy of ^{211}At-labeled GNS in an orthotopic setting. Finally, the developed GNS nanoplatform can also be applied for TAT to treat other types of cancer and through the use of different targeting ligands.

Conclusion

In summary, we have developed a novel ^{211}At radiolabeling nanoplatform using biocompatible GNS and performed the first in vivo biodistribution and ^{211}At therapy study with gold nanoparticles. Our experimental results demonstrated that the developed nanoplatform has the advantages of a simple radiolabeling process, high radiolabeling efficiency and loading capacity, minimal in vivo dissociation, and potent therapeutic effect. As a result, our novel ^{211}At nanoplatform has a great potential to be applied for future preclinical studies and clinical translation aimed at benefiting cancer patients.

Acknowledgments

The authors would like to acknowledge the support from the US National Institutes of Health (R01EB028078) and the US Department of Defense (W81XWH1910684). The content of the information in this paper does not necessarily reflect the position or the policy of the government, and no official endorsement should be inferred.

Disclosure

The authors report no conflicts of interest in this work.

References

1. Poty S, Francesconi LC, McDevitt MR, et al. Alpha-emitters for radiotherapy: from basic radiochemistry to clinical studies-Part 1. *J Nucl Med*. 2018;59(6):878–884.
2. Zalutsky MR, Vaidyanathan G. Astatine-211-labeled radiotherapeutics: an emerging approach to targeted alpha-particle radiotherapy. *Curr Pharm Des*. 2000;6(14):1433–1455.
3. Poty S, Francesconi LC, McDevitt MR, et al. Alpha-emitters for radiotherapy: from basic radiochemistry to clinical studies-Part 2. *J Nucl Med*. 2018;59(7):1020–1027.
4. Meyer GJ. Astatine. *J Labelled Comp Radiopharm*. 2018;61(3):154–164.
5. Zalutsky MR, Reardon DA, Akabani G, et al. Clinical experience with alpha-particle emitting ^{211}At: treatment of recurrent brain tumor patients with ^{211}At-labeled chimeric antitenascin monoclonal antibody 81C6. *J Nucl Med*. 2008;49(1):30–38.
6. Teze D, Sergentu DC, Kalichuk V, et al. Targeted radionuclide therapy with astatine-211: oxidative dehalogenation of astatobenzoate conjugates. *Sci Rep*. 2017;7(1):2579.
7. Choi J, Vaidyanathan G, Koumarianou E, et al. Astatine-211 labeled anti-HER2 5F7 single domain antibody fragment conjugates: radiolabeling and preliminary evaluation. *Nucl Med Biol*. 2018;56:10–20.
8. Yuan H, Khoury CG, Hwang H, et al. Gold nanostars: surfactant-free synthesis, 3D modelling, and two-photon photoluminescence imaging. *Nanotechnology*. 2012;23(7):075102.
9. Liu Y, Carpenter AB, Pirozzi CJ, et al. Non-invasive sensitive brain tumor detection using dual-modality bioimaging nanoprobe. *Nanotechnology*. 2019;30(27):275101.
10. Maeda H. Tumor-selective delivery of macromolecular drugs via the EPR effect: background and future prospects. *Bioconj Chem*. 2010;21:797–802.
11. Maeda H. The enhanced permeability and retention (EPR) effect in tumor vasculature: the key role of tumor-selective macromolecular drug targeting. *Advan Enzyme Regul*. 2001;41:189–207.
12. Ostrom QT, Gittleman H, Fulop J, et al. CBTRUS statistical report: primary brain and central nervous system tumors diagnosed in the United States in 2008-2012. *Neuro Oncol*. 2015;17(Suppl4):iv1–iv62.
13. Davis ME. Glioblastoma: overview of disease and treatment. *Clin J Oncol Nurs*. 2016;20(5 Suppl):S2–8.
14. Mariotto AB, Yabroff KR, Shao Y, et al. Projections of the cost of cancer care in the United States: 2010-2020. *J Natl Cancer Inst*. 2011;103(2):117–128.
15. Stupp R, Mason WP, van den Bent MJ, et al. Radiotherapy plus concomitant and adjuvant temozolomide for glioblastoma. *N Engl J Med*. 2005;352(10):987–996.
16. Ningaraj NS, Salimath BP, Sankpal UT, et al. Targeted brain tumor treatment-current perspectives. *Drug Target Insights*. 2007;2:197–207.
17. Krex D, Klink B, Hartmann C, et al. Long-term survival with glioblastoma multiforme. *Brain*. 2007;130:2596–2606.
18. Omuro A, DeAngelis LM. Glioblastoma and other malignant gliomas: a clinical review. *JAMA*. 2013;310(17):1842–1850.
19. Ostrom QT, Bauchet L, Davis FG, et al. The epidemiology of glioma in adults: a "state of the science" review. *Neuro-Oncology*. 2014;16(7):896–913.
20. Hartman KB, Hamlin DK, Wilbur S, et al. ^{211}AtCl@US-Tube nanocapsules: a new concept in radiotherapeutic-agent design. *Small*. 2007;3(9):1496–1499.
21. Dziawer L, Koźmiński P, Męczyńska-Wielgosz S, et al. Gold nanoparticle bioconjugates labelled with ^{211}At for targeted alpha therapy. *RSC Adv*. 2017;7:41024–41032.
22. Dziawer L, Majkowska-Pilip A, Gaweł D, et al. Trastuzumab-modified gold nanoparticles labeled with ^{211}At as a prospective tool for local treatment of HER2-positive breast cancer. *Nanomaterials*. 2019;9:632.

23. Liu Y, Chongsathidkiet P, Crawford BM, et al. Plasmonic gold nanostar-mediated photothermal immunotherapy for brain tumor ablation and immunologic memory. *Immunotherapy*. 2019;11(15):1293–1302.
24. Liu Y, Maccarini P, Palmer GM, et al. Synergistic immuno photothermal nanotherapy (SYMPHONY) for the treatment of unresectable and metastatic cancers. *Sci Rep*. 2017;7(1):8606.
25. Feng Y, Zalutsky MR. Production, purification and availability of ^{211}At: near term steps toward global access. *Nucl Med Biol*. 2021;100:12–23.
26. Demidov Y, Zaitsevskii A. Adsorption of the astatine species on a gold surface: a relativistic density functional theory study. *Chem Phys Lett*. 2018;691:126–130.
27. Zalutsky M, Stabin MG, Larsen RH, et al. Tissue distribution and radiation dosimetry of astatine-211-labeled chimeric 81C6, an α -particle-emitting immunoconjugate. *Nucl Med Biol*. 1997;24:255–261.
28. Bäck T, Andersson H, Divgi CR, et al. ^{211}At radioimmunotherapy of subcutaneous human ovarian cancer xenografts: evaluation of relative biologic effectiveness of an α-Emitter in vivo. *J Nucl Med*. 2005;46 (12):2061–2067.
29. Orozco JJ, Bäck T, Kenoyer A, et al. Anti-CD45 radioimmunotherapy using ^{211}At with bone marrow transplantation prolongs survival in a disseminated murine leukemia model. *Blood*. 2013;121(18):3759–3767.
30. Ohshima Y, Sudo H, Watanabe S, et al. Antitumor effects of radionuclide treatment using α-emitting meta-^{211}At-astatobenzylguanidine in a PC12 pheochromocytoma model. *Eur J Nucl Med Mol Imaging*. 2018;45:999–1010.
31. Dekempeneer Y, Bäck T, Aneheim E, et al. Labeling of anti-HER2 nanobodies with astatine-211: optimization and the effect of different coupling reagents on their in vivo behavior. *Mol Pharm*. 2019; 16:3524–3533.
32. Ohshima Y, Suzuki H, Hanaoka H, et al. Preclinical evaluation of new α-radionuclide therapy targeting LAT1: 2-[^{211}At]astato-α-methyl -L-phenylalanine in tumor-bearing model. *Nucl Med Biol*. 2020;90–91:15–22.
33. Makvandi M, Lee H, Puentes LN, et al. Targeting PARP-1 with alpha-particles is potently cytotoxic to human neuroblastoma in preclinical models. *Mol Cancer Ther*. 2019;18:1195–1204.
34. Liu W, Ma H, Tang Y, et al. One-step labelling of a novel small-molecule peptide with astatine-211: preliminary evaluation in vitro and in vivo. *J Radioanal Nucl Chem*. 2018;316:451–456.
35. Liu W, Tang Y, Ma H, et al. Astatine-211 labelled a small molecule peptide: specific cell killing in vitro and targeted therapy in a nude-mouse model. *Radiochim Acta*. 2021;109(2):119–126.
36. Liu Y, Ashton JR, Moding EJ, et al. A plasmonic gold nanostar theranostic probe for in vivo tumor imaging and photothermal therapy. *Theranostics*. 2015;5(9):946–960.
37. Gao N, Chen Y, Li L, et al. Shape-dependent two-photon photoluminescence of single gold nanoparticles. *J Phys Chem C*. 2014;118 (25):13904–13911.
38. Liu Y, Huang W, Xiong C, et al. Biodistribution and sensitive tracking of immune cells with plasmonic gold nanostars. *Int J Nanomedicine*. 2019;14:3403–3411.
39. Rastinehad AR, Anastos H, Wajswol E, et al. Gold nanoshell-localized photothermal ablation of prostate tumors in a clinical pilot device study. *Proc Natl Acad Sci USA*. 2019;116:18590–18596.

International Journal of Nanomedicine Dovepress

Publish your work in this journal

The International Journal of Nanomedicine is an international, peer-reviewed journal focusing on the application of nanotechnology in diagnostics, therapeutics, and drug delivery systems throughout the biomedical field. This journal is indexed on PubMed Central, MedLine, CAS, SciSearch®, Current Contents®/Clinical Medicine, Journal Citation Reports/Science Edition, EMBase, Scopus and the Elsevier Bibliographic databases. The manuscript management system is completely online and includes a very quick and fair peer-review system, which is all easy to use. Visit http://www.dovepress.com/testimonials.php to read real quotes from published authors.

Submit your manuscript here: https://www.dovepress.com/international-journal-of-nanomedicine-journal

Pacifichem 2021: A Creative Vision for the Future

Session: 180 Advancements in the Chemistry of Targeted Alpha Therapy
Organizers: Wilbur, D. Scott; Schaffer, Paul; Watanabe, Shigeki

Gold Nanoparticles as A Novel Delivery Strategy for Targeted Alpha Therapy

Yang Liu[1], Zhengyuan Zhou[2], Ganesan Vaidyanathan[2], Michael Zalutsky[1,2], Tuan Vo-Dinh[1,3,4]

1. Department of Biomedical Engineering, Duke University, NC 27708, USA
2. Department of Radiology, Duke University Medical Center, NC 27710, USA
3. Department of Chemistry, Duke University, NC 27708, USA
4. Fitzpatrick Institute for Photonics, Duke University 27708, NC, USA

Cancer is a severe threat to human health, causing more than 9 million deaths each year worldwide. There is an urgent need to develop novel therapeutic agents to substantially improve cancer treatment. With high linear energy transfer, alpha particles exhibit superior cell-killing effect as a single alpha-particle track can lead to lethal DNA double-strand breaks. In addition, the range of alpha particles in tissues is very short (less than 100 μm), allowing tumor-specific treatment with minimal collateral damage to surrounding healthy tissues. Among different available alpha-particle emitters, ^{211}At has the advantages including an optimal half-life (7.2 h) and no long-lived daughter radionuclides. Traditional approaches to incorporate ^{211}At into targeting molecules can be rather convoluted, hindering their clinical translation. We have developed a unique ^{211}At delivery strategy based on biocompatible gold nanoparticles (AuNPs). With an intrinsic strong At-Au chemical bond, it was possible to label AuNPs with ^{211}At with 97% yield simply by mixing an aqueous suspension of AuNPs with ^{211}At at room temperature for only a few minutes. The stability of the labeled AuNPs was determined by incubating in liver homogenate or serum for 2 h at room temperature. More than 96% and 98% of ^{211}At activity were associated with AuNPs in the presence of liver homogenate and serum, respectively. Using microPET/CT imaging, we also demonstrated that ^{124}I-labeled targeted AuNPs could accumulate selectively in brain tumors by the enhanced permeability and retention (EPR) using a murine intracranial brain tumor model developed with the CT2A glioblastoma brain cancer cell line. The uptake in the tumor was 16.1 %ID/g (max) from the PET/CT data. Electron microscopy and two-photon imaging confirmed that ^{211}At-labeled AuNPs penetrated through leaky brain tumor vasculature and accumulated preferentially in brain tumor tissue. These preliminary results suggest that ^{211}At-labeled AuNPs are promising agents for alpha-particle therapy and warrant future preclinical and clinical studies.